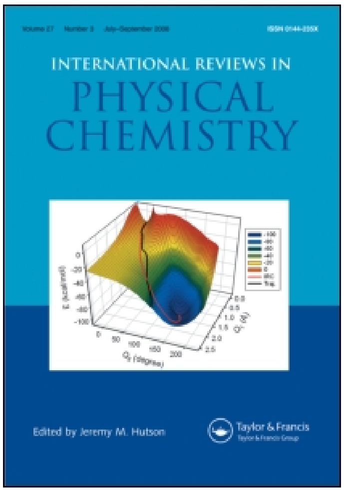

International Reviews in Physical Chemistry
Publication details, including instructions for authors and subscription information:
http://www.informaworld.com/smpp/title~content=t713724383

Nonlinear optical properties of quasilinear conjugated oligomers, polymers and organic molecules

Bernard Kirtman; Benoit Champagne

To cite this Article Kirtman, Bernard and Champagne, Benoit(1997) 'Nonlinear optical properties of quasilinear conjugated oligomers, polymers and organic molecules', International Reviews in Physical Chemistry, 16: 4, 389 — 420
To link to this Article: DOI: 10.1080/014423597230181
URL: http://dx.doi.org/10.1080/014423597230181

INTERNATIONAL REVIEWS IN PHYSICAL CHEMISTRY, 1997, VOL. 16, NO. 4, 389–420

Nonlinear optical properties of quasilinear conjugated oligomers, polymers and organic molecules

by BERNARD KIRTMAN

Department of Chemistry, University of California, Santa Barbara, California 93106, USA

and BENOIT CHAMPAGNE

Laboratoire de Chimie Theorique Appliquee, Facultes Universitaires Notre-Dame de la Paix, 61 rue de Bruxelles, B-5000 Namur, Belgium

Recent developments concerning the nonlinear optical (NLO) properties of quasilinear conjugated oligomers, polymers and organic molecules are reviewed. Although our approach is from a theoretical perspective, it is oriented towards the practical design of both second- and third-order NLO materials. Since the field is relatively new, we critically assess the current state of knowledge and indicate where further investigations are needed. Some of the topics covered, which have received limited attention in the past, are vibrational hyperpolarizabilities, the potential for enhancement of NLO response due to formation of charged structures, and the quantitative role of the solid-state medium. After the introduction there is a section on the theoretical background which presents the formal expressions that are needed, introduces the available computational methodology and points out its limitations especially when applied to large systems. Then we discuss the results that have been obtained, starting with some general elements and moving on to specifics for second- and third-order materials. There is an emphasis on *ab initio* calculations but semiempirical treatments are considered where appropriate. Finally, the concluding section deals with the important effect of intermolecular interactions.

1. Introduction

The subject of nonlinear optical (NLO) properties is attracting a great deal of interest these days. This is because there are many basic aspects that are poorly understood and many prospects for useful new optical or optoelectronic devices. Our review is oriented around the theoretical issues associated with the NLO properties of quasilinear conjugated oligomers or polymers and organic molecules; both yield solid state materials that are among the most promising in terms of practical applications. In the course of discussing the current state of knowledge in this field, many of the unresolved questions that remain will also be highlighted.

The NLO properties of a chemical system are defined as the second- and higher-order perturbation theory contributions to the dipole moment induced by a set of spatially uniform dynamic and/or static external electric fields. In the next section we begin with exact sum-over-states (SOS) expressions for the general second-order perturbation term (also known as the first hyperpolarizability) and for the general third-order perturbation term (also known as the second hyperpolarizability). These expressions involve vibronic states of the system since the fields act simultaneously on both the electronic and the vibrational motions. A convenient definition is introduced so as to formally separate the total hyperpolarizability into electronic and vibrational components.

In order to evaluate the dynamic hyperpolarizability it is common to apply what may be called the canonical or clamped-nucleus (CN) approximation. The CN approximation essentially amounts to allowing the external fields to act first on the electronic motions and then on the vibrational degrees of freedom, rather than simultaneously on both. The level of accuracy of this treatment has not been tested. However, a compact formulation of the leading correction term has now been obtained and preliminary results for a prototype molecule will be presented in section 2.

We also present in section 2 a general overview of the methods that are employed to calculate hyperpolarizabilities within the CN approximation. In principle, the *static* electronic hyperpolarizability may be determined using any of the standard methods of quantum chemistry. In practice, since we are dealing with systems that are either very large or infinite, most results have been obtained either by semiempirical procedures or by *ab initio* Hartree–Fock theory. Our emphasis will be on the latter. Recently, however, the feasibility of determining *ab initio* correlated values in a variety of cases has been demonstrated.

For dynamic electronic hyperpolarizabilities the only viable *ab initio* method for large systems, at this time, is time-dependent Hartree–Fock (TDHF) theory or, equivalently, the random-phase approximation (RPA). Approximate scaling procedures to include correlation, based on static hyperpolarizability values, have been developed and used with some success for small molecules. However, their applicability to large quasilinear conjugated systems is questionable. Multiconfiguration correlated response calculations have begun to appear for small- or medium-sized NLO chromophores.

In contrast with the electronic component, dynamic vibrational hyperpolarizabilities are no more difficult to compute than the static value. Both the static and the dynamic quantities are most often obtained using the so-called 'double harmonic oscillator' approximation wherein electrical and mechanical anharmonicities are ignored. One can include the lowest-order anharmonicity terms using a 'relaxation' technique that involves determining the equilibrium geometry as a function of the magnitude of an applied static field. This technique will be reviewed together with a perturbation treatment which yields the same terms in the form of a sum over individual modes and, in principle, also allows the calculation of higher-order anharmonicity contributions. Electron correlation can strongly alter the vibrational hyperpolarizability of small molecules and, although the question has not been addressed, it is reasonable to suppose that the same will be true for large systems as well.

As we shall see in section 3, there are three key features that characterize the NLO properties of quasilinear conjugated oligomers or polymers and organic molecules.

(1) The magnitude of the hyperpolarizability, which initially increases rapidly with the extent of conjugation, tends to be quite large.
(2) The longitudinal component of the hyperpolarizability is normally dominant.
(3) The vibrational contribution is very important.

In the past it had been thought that the vibrational hyperpolarizability determined at an optical frequency would be much less than its static value and, as a consequence, negligible compared with its electronic counterpart. Although this is true for the *linear* polarizability, and for *certain* NLO processes, it is not true in general. Thus the vibrational contribution to NLO properties can equal, or substantially exceed, the electronic contribution.

Of course, vibrational response times are slower than electronic response times because vibrational transition frequencies are less than electronic transition frequencies. How much slower depends upon the contributing vibration and can vary from a factor of roughly two to about 2000. For this reason, among others, it is desirable to characterize, as we do in section 3, the normal modes that are the major source of the vibrational NLO property. Often the vibrational response time will be much closer to the lower limit given above than the upper limit.

It is of theoretical and practical interest to understand the different chemical structure aspects that determine the magnitude of the NLO properties. Some structural features, such as the change in electron delocalization due to varying bond length alteration (BLA), play a similar qualitative role for all quasilinear π-conjugated systems. Even in this case, there may be important differences depending upon whether the source of the hyperpolarizability is vibrational or electronic. Other structural features, such as the length of the conjugated segment or the charging of the neutral system, have a property specific effect. This effect is different for the first hyperpolarizability (beta materials), where asymmetry is crucial, than for the second hyperpolarizability (gamma materials), where asymmetry is of secondary consequence. The behaviour obtained also depends upon the type of asymmetry in beta materials. All the aspects mentioned above are addressed in section 3 including the interplay between them. In addition, several other key issues, such as the nature of the repeat unit are discussed. Given the large variability that is found, we believe there are many opportunities available for designing NLO materials with desired properties.

The theoretical step from the NLO properties of an ideal isolated oligomer, polymer or organic molecule to those of a real solid-state material is a major one. This topic will be covered in section 4. It has undergone some scrutiny for beta materials in connection with the asymmetry requirement but has been, otherwise, considered only in a preliminary way for gamma materials. The very limited results available deal with nearest-neighbour interactions between small linear polyenes. These results strongly suggest that the analogous interactions between long-chain oligomers in a perfect crystalline fibre of polyacetylene would lead to a sharp reduction in both the electronic and the vibrational components of the longitudinal second hyperpolarizability. Besides the need to consider other systems, the role of more distant neighbours, of disorder and of various defects and impurities remains to be examined.

2. Theoretical background

In this section we begin with a ‘derivation’ of the CN expressions for the electronic and vibrational hyperpolarizabilities. If only the final formulae are of interest the reader may look at equations (1) and (2), refer to the text immediately below equation (4) for the definition of the vibrational and electron components, proceed to equations (8), (9 *a*) and (9 *b*) for the electronic hyperpolarizability and then to equations (24)–(27) and table 4 for the vibrational hyperpolarizabilities (in the relaxation approximation).

Our starting point is the SOS perturbation theory expressions (Orr and Ward 1971, Bishop 1993a) for the first and second hyperpolarizability generalized to include vibronic states. We use ω_1, ω_2 and ω_3 for the (circular) optical frequencies of the applied fields, $\omega_\sigma = \Sigma_i \omega_i$ for the frequency of the induced dipole moment of interest, and Greek subscripts (= x, y, z) to denote the tensor components corresponding to the frequencies ω_σ, ω_1, ω_2 and ω_3. Then the hyperpolarizabilities in the ground vibronic state may be written as

$$\beta^{\mathrm{SOS}}_{\alpha\beta\gamma}(-\omega_\sigma;\omega_1,\omega_2) = \hbar^{-2}\sum P_{-\sigma,1,2}\sum_{k,K}{}'\sum_{l,L}{}'(\omega_{kK}-\omega_\sigma)^{-1}(\omega_{lL}-\omega_2)^{-1} \times\langle 0,0|\hat{\mu}_\alpha|K,k\rangle\langle k,\ K|\bar{\hat{\mu}}_\beta|L,l\rangle\langle l,L|\hat{\mu}_\gamma|0,0\rangle, \tag{1}$$

$$\gamma^{\mathrm{SOS}}_{\alpha\beta\gamma\delta}(-\omega_\sigma;\omega_1,\omega_2,\omega_3) = \hbar^{-3}\sum P_{-\sigma,1,2,3}\Bigg(\sum_{k,K}{}'\sum_{l,L}{}'\sum_{m,M}{}'(\omega_{kK}-\omega_\sigma)^{-1}(\omega_{lL}-\omega_2-\omega_3)^{-1} \times(\omega_{mM}-\omega_3)^{-1}\langle 0,0|\hat{\mu}_\alpha|K,k\rangle\langle k,K|\overline{\hat{\mu}_\beta}|L,l\rangle\langle l,L|\overline{\hat{\mu}_\gamma}|M,m\rangle \times\langle m,M|\hat{\mu}_\delta|0,0\rangle-\sum_{k,K}{}'\sum_{l,L}{}'(\omega_{kK}-\omega_\sigma)^{-1}(\omega_{lL}-\omega_3)^{-1}(\omega_{lL}+\omega_2)^{-1} \times\langle 0,0|\hat{\mu}_\alpha|K,k\rangle\langle k,K|\hat{\mu}_\beta|0,0\rangle\langle 0,0|\hat{\mu}_\gamma|L,l\rangle\langle l,L|\hat{\mu}_\delta|0,0\rangle\Bigg), \tag{2}$$

in which $P_{-\sigma,1,2}$, for example, represents a sum over the six permutations of the pairs $(-\omega_\sigma,\hat{\mu}_\alpha)$, $(\omega_1,\hat{\mu}_\beta)$ and $(\omega_2,\hat{\mu}_\gamma)$; the vibronic wavefunction $|K,k\rangle = \phi^K_k\,\psi_K$ refers to the vibrational state ϕ^K_k determined by the potential energy surface of electronic state ψ_K; the primes on the summations indicate exclusion of the ground vibronic state ($K = 0$, $k = 0$); $\hbar\omega_{Kk}$ is the energy of state $|K,k\rangle$ relative to the ground state; $\bar{\hat{\mu}}_\xi = \hat{\mu}_\xi-\langle 0,0|\hat{\mu}_\xi|0,0\rangle$ with $\hat{\mu}_\xi$ being the electronic dipole moment operator. If $E_K(\mathbf{R}^0_K)$ is the electronic energy (including nuclear repulsion) at the equilibrium geometry of electronic state K, and ε^K_k is the vibrational energy corresponding to ϕ^K_k, then

$$\hbar\omega_{kK} = E_K(\mathbf{R}^0_K)-E_0(\mathbf{R}^0_0)+\varepsilon^K_k-\varepsilon^0_0. \tag{3}$$

The most important NLO processes correspond to the cases in which each $\omega_i = \omega$ or 0. Thus, $\beta(-\omega;\omega,0)$ refers to the dc Pockels effect and $\beta(-2\omega;\omega,\omega)$ to second harmonic generation (SHG); $\gamma(-\omega;\omega,0,0)$ corresponds to the electro-optic Kerr effect (EOKE); $\gamma(-2\omega;\omega,\omega,0)$ to dc SHG; $\gamma(-3\omega;\omega,\omega,\omega)$ to third harmonic generation (THG), and $\gamma(-\omega;\omega,\omega,-\omega)$ to either the intensity-dependent refractive index (IDRI) or degenerate four-wave mixing. Finally, note that the right-hand side of equation (2), which is the difference between two terms, may be written in the form

$$\gamma_{\alpha\beta\gamma\delta} = \gamma^{(+)}_{\alpha\beta\gamma\delta}-\gamma^{(-)}_{\alpha\beta\gamma\delta}. \tag{4}$$

It is convenient and logical to define (Bishop and Kirtman 1991) the vibrational component of β and γ by the set of terms in equations (1) and (2) where at least one of the intermediate states corresponds to the electronic ground state. The electronic component which remains is then given by the same expression except that the sum over states is changed as follows:

$$\beta^{\mathrm{SOS}}_{\mathrm{e}}:\sum_{k,K}{}'\sum_{l,L}{}'\to\sum{}'_K\sum{}'_L\sum{}_k\sum{}_l, \tag{5}$$

$$\gamma^{(+)\mathrm{SOS}}_{\mathrm{e}}:\sum_{k,K}{}'\sum_{l,L}{}'\sum_{m,M}{}'\to\sum{}'_K\sum{}'_L\sum{}'_M\sum{}_k\sum{}_l\sum{}_m;\quad \gamma^{(-)\mathrm{SOS}}_{\mathrm{e}}:\sum_{k,K}{}'\sum_{l,L}{}'\to\sum{}'_K\sum{}'_L\sum{}_k\sum{}_l. \tag{6}$$

That is to say, the sum now excludes $K = 0$, $L = 0$, $M = 0$ but within that limitation all k, l, m are allowed.

In the CN approximation (Bishop 1990, Bishop *et al.* 1997) the same perturbation theory that led to equations (5) and (6) for the electronic hyperpolarizability is employed but the nuclei are fixed at an arbitrary configuration $\mathbf{R}$. This means that vibronic states are replaced by electronic states and the energy difference $\hbar\omega_{kK}$ in equation (3) is replaced by

$$\hbar\omega_K(\mathbf{R}) = E_K(\mathbf{R}) - E_0(\mathbf{R}). \tag{7}$$

The resulting CN formulae for the electronic β (i.e. β_e^{CN}) and γ (i.e. γ_e^{CN}) become

$$\beta_e^{\mathrm{CN}}(-\omega_\sigma;\omega_1,\omega_2) = \hbar^{-2}\sum P_{-\sigma,1,2}\sum\nolimits'_K\sum\nolimits'_L \frac{\mu_\alpha^{0K}\,\bar{\mu}_\beta^{KL}\,\mu_\gamma^{L0}}{[\omega_K(\mathbf{R})-\omega_\sigma][\omega_L(\mathbf{R})-\omega_2]}, \tag{8}$$

$$\gamma_e^{(+)\mathrm{CN}}(-\omega_\sigma;\omega_1,\omega_2,\omega_3) =$$
$$\hbar^{-3}\sum P_{-\sigma,1,2,3}\sum\nolimits'_K\sum\nolimits'_L\sum\nolimits'_M \frac{\mu_\alpha^{0K}\,\bar{\mu}_\beta^{LK}\,\bar{\mu}_\gamma^{LM}\,\mu_\delta^{M0}}{[\omega_K(\mathbf{R})-\omega_\sigma][\omega_L(\mathbf{R})-\omega_2-\omega_3][\omega_M(\mathbf{R})-\omega_3]}, \tag{9a}$$

$$\gamma_e^{(-)\mathrm{CN}}(-\omega_\sigma;\omega_1,\omega_2,\omega_3) =$$
$$\hbar^{-3}\sum P_{-\sigma,1,2,3}\sum\nolimits'_K\sum\nolimits'_L \frac{\mu_\alpha^{0K}\,\mu_\beta^{K0}\,\mu_\gamma^{0L}\,\mu_\delta^{L0}}{[\omega_K(\mathbf{R})-\omega_\sigma][\omega_L(\mathbf{R})-\omega_3][\omega_L(\mathbf{R})+\omega_2]}, \tag{9b}$$

where $\mu_\alpha^{KL} = \langle K|\hat{\mu}_\alpha|L\rangle$ and $\bar{\mu}^{KL} = \mu^{KL} - \mu^{00}\,\delta_{KL}$. It is important to remember that the quantities in equations (8), (9*a*) and (9*b*) are really electronic hyperpolarizability functions since the numerators and denominators both depend upon the nuclear configuration $\mathbf{R}$. In order to obtain a specific numerical value for comparison with experiment, one evaluates equations (8), (9*a*) and (9*b*) at $\mathbf{R}_0^0$ and adds a correction due to zero-point vibrational averaging (ZPVA) over ϕ_0^0. If the hyperpolarizability function is expanded as a power series in $\mathbf{Q} = \mathbf{R} - \mathbf{R}_0^0$, the linear terms do not contribute to the ZPVA provided that anharmonicities in the vibrational potential energy surface are neglected. Thus, in the double-harmonic-oscillator approximation, the CN electronic hyperpolarizability is just the value at $\mathbf{R}_0^0$. Formulae for corrections up to second order due to anharmonicity have been given (Spackman 1996).

Although we expect the CN approximation to be reasonable it is important to know how accurately it reproduces the exact SOS electronic hyperpolarizability. To this end a first-order treatment of the difference between the two has been developed (Bishop *et al.* 1997) based on the approximation that energy differences due to nuclear motions are small compared with those associated with electronic motions. In terms of vibronic states this means that (cf. equation (3)) $\varepsilon_k^K - \varepsilon_0^0 \ll E_K(\mathbf{R}_K^0) - E_0(\mathbf{R}_0^0)$ and therefore

$$[E_K(\mathbf{R}_K^0) - E_0(\mathbf{R}_0^0) + \varepsilon_k^K - \varepsilon_0^0]^{-1} \approx [E_K(\mathbf{R}_K^0) - E_0(\mathbf{R}_0^0)]^{-1}\left(1 - \frac{\varepsilon_k^K - \varepsilon_0^0}{E_K(\mathbf{R}_K^0) - E_0(\mathbf{R}_0^0)}\right). \tag{10}$$

It is also assumed that the analogous inequality holds when $\varepsilon_k^K - \varepsilon_0^0$ is replaced by $[E_K(\mathbf{R}) - E_K(\mathbf{R}_K^0)] - [E_0(\mathbf{R}) - E_0(\mathbf{R}_0^0)]$. The resulting expressions, which will be presented elsewhere, have been evaluated (as a test case) for the longitudinal β_e of the prototype push–pull polyene system, $NH_2{-}(CH{=}CH)_3{-}NO_2$. Only single-excitation configurations (based on a restricted Hartree–Fock (RHF)/6-31G ground state) were considered and these yield just two excited electronic states (the first and sixth in order of increasing energy) that turn out to be significant. They give a first-order correction to β_e which is less than 0·02% of the canonical value.

The frequency dependence of the CN electronic hyperpolarizabilities can be calculated, in principle, from equations (8), (9*a*) and (9*b*). For large molecules such calculations are currently feasible at the *ab initio* level only by making approximations that lead to the uncoupled Hartree–Fock (UCHF) or coupled Hartree–Fock (CHF) method. Furthermore, at low frequencies there are *exact* dispersion formulas (Bishop and De Kee 1996a, b) relating the diagonal component (as well as the average value) of one NLO process to another (from this point on we omit the superscript CN on all canonical/clamped nucleus quantities), for example

$$\gamma_e(-\omega_\sigma;\omega_1,\omega_2,\omega_3) = \gamma_e(0)[1+A\omega_L^2+\ldots]. \tag{11}$$

Here $\gamma_e(0)$ is the static value, A is a constant that does not depend on the process, and $\omega_L^2 = \omega_\sigma^2+\omega_1^2+\omega_2^2+\omega_3^2$. (An exactly analogous formula, with a different constant, pertains to β_e.) For the major NLO processes $\omega_L^2 = k\omega^2$ with $k(\text{EOKE}) = 2$, $k(\text{IDRI}) = 4$, $k(\text{dc SHG}) = 6$ and $k(\text{THG}) = 12$. With $A > 0$, the electronic second hyperpolarizabilities occur in the order THG > dc SHG > IDRI > EOKE at low frequencies. The expansion in equation (11) has been extended to higher order, but the coefficient of ω^4 (and ω^6) is no longer the same for all four major NLO processes. We shall be especially interested in the longitudinal component since it is dominant for most of the systems discussed in this review.

It has been suggested that the CHF value might give a reasonably accurate result for the constant A in equation (11) or, in general (Sekino and Bartlett 1991), for the ratio $\gamma_e(-\omega_\sigma;\omega_1,\omega_2,\omega_3)/\gamma_e(0)$ at non-resonant optical frequencies. If that were the case, then one could use the correlated $\gamma_e(0)$ to obtain a correlated $\gamma_e(-\omega_\sigma;\omega_1,\omega_2,\omega_3)$. Tests on a number of small molecules have had some success (Sekino and Bartlett 1993) but, when used on a π-conjugated system (*trans*-butadiene), this scaling technique did not fare so well for the EOKE (see §3.3).

The SOS formalism, within the CN approximation, has been widely applied in semiempirical calculations of electronic hyperpolarizabilities. However, other formalisms are preferred in *ab initio* calculations. The most common *ab initio* treatment is the CHF approximation (the simpler UCHF method is equivalent to an SOS–CN calculation based on the Hartree–Fock ground state). Details of the CHF procedure may vary but the general idea is as follows (Karna and Dupuis 1991, Sekino and Bartlett 1986, 1992). A term which represents the interaction between an external electric field and the instantaneous molecular dipole is added to the ordinary Hartree–Fock one-electron potential. This field, of magnitude F, must contain both dc and optical components in order to describe the various optical processes mentioned below equation (3). The TDHF equation is then expanded as a power series in F and solved self-consistently order by order. In this way field-induced electron reorganization effects are taken into account. Finally, each hyperpolarizability is obtained by calculating the appropriate frequency-dependent term in the expression for the induced dipole moment.

In the static field limit, the above calculation corresponds to an analytical differentiation of the time-independent Hartree–Fock dipole moment with respect to F. The Hartree–Fock dipole moment, in turn, may be obtained as an expectation value or, equivalently, as the negative first derivative of the field-dependent energy. Thus the first hyperpolarizability is proportional to the third derivative of the energy, or the second derivative of the dipole moment, or the first derivative of the linear polarizability. In the so-called finite-field treatment the energy, dipole moment or linear polarizability is determined analytically as a function of field and the remaining differentiations are done numerically.

The finite-field approach is also the simplest way to incorporate electron correlation in the static field limit. However, for non-variational methods such as

Table 1. Vibrational hyperpolarizability contributions from equations (1) and (2). Reprinted with permission from Bishop and Kirtman (1991). Copyright 1991 American Institute of Physics.

Symbol	Formula
Equation (1)	
$[\mu\alpha]$	$\beta_{\alpha\beta\gamma}(K = 0, L \neq 0) + \beta_{\alpha\beta\gamma}(K \neq 0, L = 0)$
$[\mu^3]$	$\beta_{\alpha\beta\gamma}(K = 0, L = 0)$
Equation (2)	
$[\alpha^2]$	$\gamma^{(+)}_{\alpha\beta\gamma\delta}(K \neq 0, L = 0, M \neq 0)$
$[\mu\beta]$	$\gamma^{(+)}_{\alpha\beta\gamma\delta}(K = 0, L \neq 0, M \neq 0) + \gamma^{(+)}_{\alpha\beta\gamma\delta}(K \neq 0, L \neq 0, M = 0)$
$[\mu^2\alpha]$	$\gamma^{(+)}_{\alpha\beta\gamma\delta}(K = 0, L = 0, M \neq 0) + \gamma^{(+)}_{\alpha\beta\gamma\delta}(K = 0, L \neq 0, M = 0)$ $+ \gamma^{(+)}_{\alpha\beta\gamma\delta}(K \neq 0, L = 0, M = 0) - \gamma^{(-)}_{\alpha\beta\gamma\delta}(K = 0, L \neq 0) - \gamma^{(-)}_{\alpha\beta\gamma\delta}(K \neq 0, L = 0)$
$[\mu^4]$	$\gamma^{(+)}_{\alpha\beta\gamma\delta}(K = 0, L = 0, M = 0) - \gamma^{(-)}_{\alpha\beta\gamma\delta}(K = 0, L = 0)$

perturbation theory or coupled-cluster theory, the expectation value of the dipole moment is not the same as the negative of the energy derivative. In these cases numerical differentiation of the energy is preferred (Sasagne *et al.* 1993). Quantum chemistry programs now routinely include a provision for obtaining the energy in an applied static electric field.

It is much more difficult to use frequency-dependent fields. Several different procedures for dealing with this problem have been presented. One of these is the pseudo-energy derivative method of Rice and Handy (1991) or the related quasi-energy derivative method of Itoh and coworkers (Sasagne *et al.* 1993, Aiga *et al.* 1993); another is the equations of motion (with coupled clusters) procedure of Stanton and Bartlett (1993). The latter has been used (Sekino and Bartlett 1995) to obtain the EOKE value for *trans*-butadiene which, as noted above, reveals a significant error in the scaling technique for estimating the effect of electron correlation on frequency dispersion. There are two other formulations that are more closely akin to SOS–CN. The frequency-dependent moment method (Iwata 1983) is, in fact, an equivalent procedure. It is obtained by rewriting the SOS hyperpolarizability expression in terms of solutions to simultaneous equations and thereby, circumventing the computationally intensive diagonalization of the complete configuration interaction (CI) matrix. The other is based on the polarization propagator (Linderberg and Öhrn 1973, Olsen and Jørgensen 1985, Oddershede 1987). It recasts the SOS hyperpolarizability into the form of a superoperator resolvent whose poles and residues determine the entire frequency spectrum. Large-scale calculations are required even at the lowest level (RPA) which is equivalent to TDHF. Nonetheless, in contrast with the previously mentioned approaches, *ab initio* applications to small or medium-sized (up to ten second-row atoms) NLO chromophores including electron correlation have begun to appear (Jaszunski *et al.* 1993, Mikkelsen *et al.* 1994).

The terms in equations (1) and (2) that contribute to the vibrational hyperpolarizability are those where at least one of the electronic state indices K, L, M is zero. They are listed in table 1 using a square-bracket notation which will be obvious as we go on. In that notation,

$$\beta^{\mathrm{v}}_{\alpha\beta\gamma}(-\omega_\sigma; \omega_1, \omega_2) = [\mu\alpha] + [\mu^3] \tag{12}$$

and

$$\gamma^{\mathrm{v}}_{\alpha\beta\gamma\delta}(-\omega_\sigma; \omega_1, \omega_2, \omega_3) = [\alpha^2] + [\mu\beta] + [\mu^2\alpha] + [\mu^4], \tag{13}$$

Table 2. Vibrational hyperpolarizability contributions. The vibrational dipole transition matrix elements in the electronic ground state are denoted $(\mu_\alpha)_{0k} = \langle 0|\mu_\alpha|k\rangle$, $(a \pm b)^{-1} \equiv (a+b)^{-1} + (a-b)^{-1}$ and $(a \pm b)^{-1}(c \pm d)^{-1} \equiv (a+b)^{-1}\ (c+d)^{-1} + (a-b)^{-1}\ (c-d)^{-1}$. Reprinted with permission from Bishop and Kirtman (1991). Copyright 1991 American Institute of Physics.

Symbol	Formula
$[\mu\alpha]$	$\frac{1}{2}\hbar^{-1}\sum P_{-\sigma,1,2}\sum_k{}'(\mu_\alpha)_{0k}(\alpha_{\beta\gamma})_{k0}(\omega_k \pm \omega_\sigma)^{-1}$
$[\mu^3]$	$\hbar^{-2}\sum P_{-\sigma,1,2}\sum_k{}'\sum_l{}'(\mu_\alpha)_{0k}(\bar{\mu}_\beta)_{kl}(\mu_\gamma)_{l0}(\omega_k - \omega_\sigma)^{-1}(\omega_l - \omega_2)^{-1}$
$[\alpha^2]$	$\frac{1}{4}\hbar^{-1}\sum P_{-\sigma,1,2,3}\sum_k{}'(\alpha_{\alpha\beta})_{0k}(\alpha_{\gamma\delta})_{k0}(\omega_k - \omega_2 - \omega_3)^{-1}$
$[\mu\beta]$	$\frac{1}{6}\hbar^{-1}\sum P_{-\sigma,1,2,3}\sum_k{}'(\mu_\alpha)_{0k}(\beta_{\beta\gamma\delta})_{k0}(\omega_k \pm \omega_\sigma)^{-1}$
$[\mu^2\alpha]$	$\frac{1}{2}\hbar^{-2}\sum P_{-\sigma,1,2,3}\sum_k{}'\sum_l{}'\{(\mu_\alpha)_{0k}(\bar{\mu}_\beta)_{kl}(\alpha_{\gamma\delta})_{l0}(\omega_k \pm \omega_\sigma)^{-1}[\omega_l \pm (\omega_2 + \omega_3)]^{-1}$ $+ (\mu_\alpha)_{0k}(\bar{\alpha}_{\beta\gamma})_{kl}(\mu_\delta)_{l0}(\omega_k - \omega_\sigma)^{-1}(\omega_l - \omega_3)^{-1}\}$
$[\mu^4]$	$\hbar^{-3}\sum P_{-\sigma,1,2,3}\Big(\sum_k{}'\sum_l{}'\sum_m{}'(\mu_\alpha)_{0k}(\bar{\mu}_\beta)_{kl}(\bar{\mu}_\gamma)_{lm}(\mu_\delta)_{m0}$ $\times(\omega_k - \omega_\sigma)^{-1}(\omega_l - \omega_2 - \omega_3)^{-1}(\omega_m - \omega_3)^{-1}$ $-\sum_k{}'\sum_l{}'(\mu_\alpha)_{0k}(\mu_\beta)_{k0}(\mu_\gamma)_{0l}(\mu_\delta)_{l0}(\omega_k - \omega_\sigma)^{-1}(\omega_l - \omega_3)^{-1}(\omega_l - \omega_2)^{-1}\Big)$

where $\gamma^{\mathrm{v}} = \gamma^{(+)\mathrm{v}} - \gamma^{(-)\mathrm{v}}$. In the CN approximation the nuclei are fixed at $\mathbf{R}$ in all electronic states with the exception of the ground state. Thus, equation (7) is again employed instead of equation (3) unless $K = 0$, in which case we have

$$\hbar\omega_{k0} = \varepsilon_k^0 - \varepsilon_0^0. \tag{14}$$

A first-order treatment of the difference between the SOS and CN vibrational hyperpolarizability has been developed (Bishop *et al.* 1997) along the same lines as the electronic hyperpolarizability discussed earlier. Again, we note that the resulting formulae will be reported elsewhere. The test calculation on $NH_2{-}(CH{=}CH)_3{-}NO_2$ described below equation (10) has been extended to the vibrational β arising from the nine most important normal modes. In this case, the first-order correction due to the difference between SOS and CN values for those modes is less than 2%.

Under non-resonant conditions the expressions for the CN vibrational hyperpolarizability can be simplified by neglecting optical frequencies in comparison with electronic transition frequencies. Then, by applying the closure relation $\sum_k |k\rangle\langle k| = 1$ for the nuclear degrees of freedom, one can derive (Bishop and Kirtman 1991) the formulae shown in table 2 for the square brackets in equations (12) and (13). These formulae are given in terms of the CN static electronic properties in the ground electronic states:

$$\alpha_{\alpha\beta} = \alpha^{\mathrm{e}}_{\alpha\beta} = \hbar^{-1}\sum P_{-\sigma,1}\sum{}'_K \frac{\mu_\alpha^{0K}\mu_\beta^{K0}}{\omega_K(\mathbf{R})}, \tag{15}$$

$$\beta_{\alpha\beta\gamma} = \beta^{\mathrm{e}}_{\alpha\beta\gamma} = \hbar^{-2}\sum P_{-\sigma,1,2}\sum{}'_K\sum{}'_L \frac{\mu_\alpha^{0K}\bar{\mu}_\beta^{KL}\mu_\gamma^{L0}}{\omega_K(\mathbf{R})\omega_L(\mathbf{R})}, \tag{16}$$

Table 3. Non-zero terms (√) in the perturbation expansion of the square-bracket contributions to the vibrational hyperpolarizability. $[\mu\alpha]$ and $[\mu^3]$ determine β^{v}; the remaining square brackets determine γ^{v}. Reprinted with permission from Bishop and Kirtman (1991). Copyright 1991 American Institute of Physics.

	(n,m)				
	(0,0)	(1,0)	(2,0)	(0,1)	(1,1)
$[\mu\alpha]$	√		√		√
$[\mu^3]$		√		√	
$[\alpha^2]$	√		√		√
$[\mu\beta]$	√		√		√
$[\mu^2\alpha]$		√		√	
$[\mu^4]$			√		√

and $\mu_\alpha = \mu_\alpha^{\mathrm{e}} = \mu_\alpha^{00}(\mathbf{R})$. Equation (16) is obtained from equation (8) simply by setting the optical frequencies ω_2, ω_σ equal to zero; equation (15) follows from the usual CN expression for the linear polarizability in a similar manner.

One way of evaluating the CN vibrational hyperpolarizability is to expand the electrical properties μ, α, β as a power series in the normal coordinates $\mathbf{Q}$ and to do the same for the vibrational potential that determines the vibrational wavefunctions ϕ_k. In the case of the linear polarizability, for instance

$$\alpha_{\xi\eta}^{\mathrm{e}} = \alpha_{\xi\eta}^{0} + \sum_{a} (\xi\eta/a)\, Q_a + \tfrac{1}{2} \sum_{a,\,b} (\xi\eta/ab)\, Q_a Q_b + \dots, \tag{17}$$

where $(\xi\eta/a) = (\partial\alpha_{\xi\eta}/\partial Q_a)$, $(\xi\eta/ab) = (\partial^2\alpha_{\xi\eta}/\partial Q_a \partial Q_b)$. The harmonic approximation is obtained by including the constant term as well as those that are linear in $\mathbf{Q}$. From a perturbation theory perspective the terms quadratic in $\mathbf{Q}$ are considered to be first order in electrical anharmonicity, those that are cubic are considered to be second order, etc. Similarly, the vibrational potential in expanded form is

$$V = V^0 + \tfrac{1}{2} \sum_{a} \omega_a^2 Q_a^2 + \tfrac{1}{6} \sum_{a,\,b,\,c} F_{a,\,b,\,c} Q_a Q_b Q_c + \dots . \tag{18}$$

In this case the harmonic approximation is obtained by truncating the series after the quadratic terms (the linear terms vanish at the equilibrium geometry). The cubic terms are considered to be first order in mechanical anharmonicity, the quartic terms are second order, and so forth.

The various square-bracket contributions may be determined by means of ordinary double-perturbation theory which gives $[\;] = \Sigma_n \Sigma_m [\;]^{n,\,m}$ with n equal to the order in electrical anharmonicity and m the order in mechanical anharmonicity. On the basis of symmetry and other arguments about half of the $[\;]^{n,\,m}$ vanish. Those that remain in low order are listed (Kirtman and Bishop 1990, Bishop and Kirtman 1991) in table 3. Note that in the harmonic approximation ($n = m = 0$) the first hyperpolarizability consists of just a single $[\mu\alpha]^{0,0}$ term and the second hyperpolarizability is the sum of two square-bracket terms $[\alpha^2]^{0,0}$ and $[\mu\beta]^{0,0}$. Formulae for these terms, as well as the $n = 1$, $m = 0$ and $n = 0$, $m = 1$ contributions, may be found in table 4. Compact expressions for $n = 1$, $m = 1$ and $n = 2$, $m = 0$ are also available in the literature (Bishop and Kirtman 1991).

Each perturbation term in table 4 is written as a sum over normal modes. In order

Table 4. Compact formulae for low-order dynamic vibrational hyperpolarizabilities. The notation $\lambda_x^{\pm i} = (\omega_x + \omega_i)^{-1}(\omega_x - \omega_i)^{-1}$, $\lambda_x^{\pm ij} = (\omega_x + \omega_i + \omega_j)^{-1}(\omega_x - \omega_i - \omega_j)^{-1}$ has been employed. Here ω_x is a vibrational circular frequency; ω_i *and* ω_j are optical circular frequencies. Reprinted with permission from Bishop and Kirtman (1992). Copyright 1992 American Institute of Physics.

β^{v}	
	$[\mu\alpha]^{0,0} = \frac{1}{2}\sum P_{-\sigma,1,2}\sum_{a}(\alpha/a)(\beta\gamma/a)\lambda_a^{\pm\sigma}$
	$[\mu^3]^{1,0} = \frac{1}{2}\sum P_{-\sigma,1,2}\sum_{a,b}(\alpha/a)(\beta/ab)(\gamma/b)\lambda_a^{\pm\sigma}\lambda_b^{\pm 2}$
	$[\mu^3]^{0,1} = -\frac{1}{6}\sum P_{-\sigma,1,2}\sum_{a,b,c}F_{abc}(\alpha/a)(\beta/b)(\gamma/c)\lambda_a^{\pm\sigma}\lambda_b^{\pm 1}\lambda_c^{\pm 2}$
γ^{v}	
	$[\alpha^2]^{0,0} = \frac{1}{8}\sum P_{-\sigma,1,2,3}\sum_{a}(\alpha\beta/a)(\gamma\delta/a)\lambda_a^{\pm 23}$
	$[\mu\beta]^{0,0} = \frac{1}{6}\sum P_{-\sigma,1,2,3}\sum_{a}(\alpha/a)(\beta\gamma\delta/a)\lambda_a^{\pm\sigma}$
	$[\mu^2\alpha]^{1,0} = \frac{1}{4}\sum P_{-\sigma,1,2,3}\sum_{a,b}((\alpha/a)(\beta\gamma/ab)(\delta/b)\lambda_a^{\pm\sigma}\lambda_b^{\pm 3} + 2(\alpha/a)(\beta/ab)(\gamma\delta/b)\lambda_b^{\pm 23})$
	$[\mu^2\alpha]^{0,1} = -\frac{1}{4}\sum P_{-\sigma,1,2,3}\sum_{a,b,c}F_{abc}(\alpha/a)(\beta/b)(\gamma\delta/c)\lambda_a^{\pm\sigma}\lambda_b^{\pm 1}\lambda_c^{\pm 23}$

to evaluate these terms at the harmonic level of approximation, one needs to know the first derivatives of μ, α and β with respect to normal coordinates as well as the harmonic vibrational frequencies. For the systems of interest here the vibrational properties (normal coordinates and frequencies) and the electrical properties μ,α and β are most often determined at the *ab initio* Hartree–Fock level. This is a compromise between semiempirical methods that can be unreliable (Champagne *et al.* 1994) and computationally demanding correlated *ab initio* treatments. For the electrical properties, this means replacing equations (15) and (16) by the CHF approximation. Judging from small molecules (Bishop *et al.* 1993) the omitted correlation effects could be quite important. Although analytical CHF normal coordinate derivatives of μ and α are available in standard quantum chemistry programs, the derivatives of β must be obtained either by the finite-field method applied to (α/a) or by finite nuclear displacements applied to β. For mechanical and electrical anharmonicity contributions, finite nuclear displacements are required to evaluate the cubic vibrational force constants and electrical property second derivatives. This is sufficiently tedious so that no results for NLO materials have yet been reported.

Recently, an alternative (somewhat more approximate) method (Bishop *et al.* 1995), that circumvents the direct calculation of cubic force constants and electrical property derivatives with respect to normal coordinates, has been developed and tested (Bishop and Dalskov 1996). This method simply requires obtaining α and β in the presence of a uniform static electric field with and without allowing the nuclei to relax to equilibrium positions when the field is present. One defines

$$(\Delta P)_{\mathbf{R}_F} = P(F, \mathbf{R}_F) - P(0, \mathbf{R}_0), \tag{19}$$

where P is one of the electrical properties and $\mathbf{R}_F$ is the equilibrium geometry for a static field F. Then it is easy to show that

$$\begin{aligned} (\Delta\alpha_{\alpha\beta})_{\mathbf{R}_F} &= b_2 F_\gamma + \tfrac{1}{2} g_2 F_\gamma F_\delta + \dots . \\ (\Delta\beta_{\alpha\beta\gamma})_{\mathbf{R}_F} &= g_3 F_\delta + \dots , \end{aligned} \tag{20}$$

with

$$\begin{aligned} b_2 &= \beta^{\mathrm{e}}_{\alpha\beta\gamma}(0;0,0) + \beta^{\mathrm{v(r)}}_{\alpha\beta\gamma}(-\omega;\omega,0)_{\omega\to\infty}, \\ g_2 &= \gamma^{\mathrm{e}}_{\alpha\beta\gamma\delta}(0;0,0,0) + \gamma^{\mathrm{v(r)}}_{\alpha\beta\gamma\delta}(-\omega;\omega,0,0)_{\omega\to\infty}, \end{aligned} \tag{21}$$

$$g_3 = \gamma^{\mathrm{e}}_{\alpha\beta\gamma\delta}(0;0,0,0) + \gamma^{\mathrm{v(r)}}_{\alpha\beta\gamma\delta}(-2\omega;\omega,\omega,0)_{\omega\to\infty} \tag{22}$$

and

$$\begin{aligned} \bar{\gamma}^{\mathrm{v(r)}}(-\omega;\omega,\omega,-\omega)_{\omega\to\infty} = 4[&\bar{\gamma}^{\mathrm{v(r)}}(-\omega;\omega,0,0)_{\omega\to\infty} \\ &-\tfrac{4}{3}\bar{\gamma}^{\mathrm{v(r)}}(-2\omega;\omega,\omega,0)_{\omega\to\infty} - \tfrac{1}{6}\bar{\gamma}^{\mathrm{v(r)}}(0;0,0,0)]. \end{aligned} \tag{23}$$

In equations (21)–(23) the superscript (r) has been added to indicate that only those perturbation terms that arise from the geometry relaxation due to the static field, namely $[\,]^{0,0} + [\,]^{1,0} + [\,]^{0,1}$ are included. The subscript $\omega \to \infty$ denotes that these terms are obtained in the 'infinite-(optical-)frequency' limit, which corresponds to retaining the 'enhanced' contributions of Elliott and Ward (1984) and yields the dominant part at ordinary optical frequencies. Whereas equations (21) and (22) are valid for all tensor components, equation (23) is valid only for the diagonal components (or for the mean value) which is the reason for the overbar. Note that neither $\beta^{\mathrm{v}}(-2\omega;\omega,\omega)$ nor $\gamma^{\mathrm{v}}(-3\omega;\omega,\omega,\omega)$ can be found by this method. Indeed, the vibrational SHG and THG both vanish in the 'infinite-frequency' approximation.

The 'infinite-frequency' approximation implies that the dispersion of the dynamic vibrational hyperpolarizability is small (for a given process) in the optical region of the spectrum. On the other hand, there may be significant variations in the 'infinite-frequency' value for different processes according to the above discussion. As the frequency is lowered, the dispersion eventually increases so that all processes yield the same value in the static limit. It turns out, at least for diagonal components (and average values), that the square-bracket terms in the 'infinite-frequency' expressions are simple fractional multiples of the corresponding square-bracket terms in the static limit. If we let $[\,]_{\omega=0}$ designate the static limit, then it is easily demonstrated (Kirtman *et al.* 1996) for the diagonal components that

$$\beta^{\mathrm{v(r)}}(-\omega;\omega,0)_{\omega\to\infty} = \tfrac{1}{3}[\mu\alpha]^{0,0}_{\omega=0}, \quad \beta^{\mathrm{v(r)}}(-2\omega;\omega,\omega)_{\omega\to\infty} = 0, \tag{24}$$

$$\gamma^{\mathrm{v(r)}}(-\omega;\omega,0,0,)_{\omega\to\infty} = \tfrac{1}{2}[\mu\beta]^{0,0}_{\omega=0} + \tfrac{1}{3}[\alpha^2]^{0,0}_{\omega=0} + \tfrac{1}{6}[\mu^2\alpha]^{0,1}_{\omega=0} + \tfrac{1}{6}[\mu^2\alpha]^{1,0}_{\omega=0}, \tag{25}$$

$$\gamma^{\mathrm{v(r)}}(-2\omega;\omega,\omega,0)_{\omega\to\infty} = \tfrac{1}{4}[\mu\beta]^{0,0}_{\omega=0}, \quad \gamma^{\mathrm{v(r)}}(-3\omega;\omega,\omega,\omega)_{\omega\to\infty} = 0, \tag{26}$$

$$\gamma^{\mathrm{v(r)}}(-\omega;\omega,\omega,-\omega)_{\omega\to\infty} = \tfrac{2}{3}[\alpha^2]^{0,0}_{\omega=0}. \tag{27}$$

As noted earlier, the longitudinal component will dominate for most of the systems discussed in this review. In that event, equations (24)–(27) may be employed directly. It has also been shown (Bishop and Dalskov 1996) that analogous relations hold for the average quantities.

3. Application to quasilinear conjugated oligomers or polymers and organic molecules

3.1. *Some general considerations*

Consider, as an example, the set of linear polyenes C_4H_6, C_6H_8, C_8H_{10}, ..., $C_{2N}H_{2N+2}$ in the all-*trans* configuration. Since these oligomers are centrosymmetric, the first hyperpolarizability will vanish. Calculations of the static longitudinal second electronic hyperpolarizability at the CHF/6-31G level yield (Kirtman *et al.* 1995)

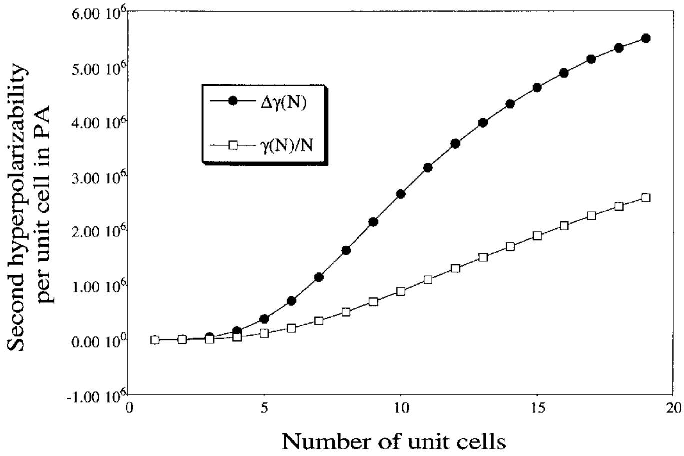

Figure 1. Static longitudinal electronic second hyperpolarizability $\gamma_L^e(0)$ per unit cell as a function of chain length in PA chains. The two alternative definitions of the unit cell property, i.e. $\Delta\gamma(N) = [\gamma_L^e(0)]_{N+1} - [\gamma_L^e(0)]_N$ and $\gamma(N)/N = \gamma_L^e(0)/N$ are compared. These are CHF/6-31G results in au.

$\gamma_L^e(0)/N = 0{\cdot}3,\ 1{\cdot}8,\ 5{\cdot}4,\ 12{\cdot}0,\ \ldots \times 10^4$ au for $N = 2, 3, 4, 5, \ldots$. In comparison, the (previously unreported) values for the corresponding saturated polyethylene ($C_{2N}H_{4N+2}$) oligomers are $\gamma_L^e(0)/N = 1{\cdot}3\ ,1{\cdot}9,\ 2{\cdot}3,\ 2{\cdot}6,\ \ldots \times 10^3$au. Clearly, $\gamma_L^e(0)$ per carbon atom grows much more rapidly with increasing chain length for the linear polyenes than the saturated polyethylenes. For the latter, one can already see the saturation towards the infinite polymer value at small N. The different behaviour of the linear polyenes is due to the electron delocalization associated with π conjugation.

As the linear polyene chain is extended, the monotonically increasing plot of $\gamma_L^e(0)/N$ against N will eventually saturate to the infinite polymer, that is polyacetylene (PA), limit which is three orders of magnitude greater than the corresponding polyethylene value. If one is interested just in this limit, then a plot of $[\gamma_L^e(0)]_{N+1} - [\gamma_L^e(0)]_N$ against N will converge much more rapidly (figure 1) to the same result because chain end effects tend to cancel in taking the difference. For short polyene oligomers, other components of the second hyperpolarizability tensor may be comparable with $\gamma_L^e(0)$, although they are all smaller even for butadiene. However, the longitudinal component quickly becomes dominant with increasing N.

Details may vary according to the basis set, treatment of electron correlation and the particular system, but the behaviour just described is general for the second electronic hyperpolarizability of all quasilinear conjugated centrosymmetric oligomers. For obvious reasons these are known as gamma or third-order NLO materials. In order to generate a first hyperpolarizability, one must remove the centre of symmetry. Starting with a centrosymmetric oligomer this can be done most simply by capping one end with a donor (D) group and the other with an acceptor (A) group. Two D–A pairs that are often used are NH_2–NO_2 and $N(CH_3)_2$–CHO. Another possibility is to replace the symmetric repeat unit of the oligomer by an asymmetric unit. An example of the latter is $-(CH{=}N)-$, which is isoelectronic with $-(CH{=}CH)-$. There are, of course, other types of asymmetric structure but the two mentioned above are those that will be considered in this review. Both contain oligomeric segments; so it is meaningful to talk about the dependence of the static longitudinal electronic first hyperpolarizability $\beta_L^e(0)$ on the chain length. For beta (or second-order) NLO materials as opposed to gamma materials, the solid state packing is of paramount importance. If the three-dimensional architecture is centrosymmetric, it will destroy the second-order NLO response.

The evolution of $\beta_L^e(0)$ with increasing chain length is determined by the asymmetry as well as the electron delocalization. In contrast with $\gamma_L^e(0)/N$ we shall see that the magnitude of $\beta_L^e(0)/N$ in general goes through a maximum as the number of monomer units is increased. In particular, when an asymmetric repeat unit is involved, the sign of $\beta_L^e(0)$ may be different for long chains from that for short chains and the pure longitudinal component may not become dominant until the chain is quite long.

Roughly speaking, the static vibrational hyperpolarizabilities of the quasilinear conjugated (and other) species that have been examined are often of the same order of magnitude as the corresponding static electronic hyperpolarizabilities. This has led to the suggestion (Castiglioni *et al.* 1996) that both properties may have the same underlying physical origin. Indeed, we know that the degree of BLA in these systems is the critical determinant of the electronic delocalization. By definition, the so-called (Castiglioni *et al.* 1993) effective conjugation coordinate (ECC) is the vibrational motion associated with the BLA and, in the few cases that have been tested, this motion makes the leading contribution to the vibrational hyperpolarizability. The smaller the BLA, the greater is the electronic delocalization and, by the same token, the larger is the effect on delocalization due to the ECC vibrational motion. Thus the static electronic and vibrational contributions to the hyperpolarizability will *tend* to vary in tandem.

Despite the qualitative connection just described, a simple quantitative relationship has not been successfully formulated (Bishop and Kirtman 1997). In fact, new calculations on prototype beta materials (see section 3.2) reveal that this relationship depends significantly upon the nature and the length of the oligomer that links the D–A pair. The dependence on the strength of the D–A pair has yet to be examined.

So far our discussion pertains specifically to neutral species. It is well known that the gamma materials discussed in this review can be charged in the solid state by doping with an electron donor or acceptor (and by other means as well). The electrical conductivity associated with the localized geometric structure that is formed about the charge on the chain has been investigated extensively, but not the NLO response. Initial calculations, as well as speculation based on related studies, indicate (cf. section 3.3) that the resulting electronic and vibrational $\gamma_L(0)$ may be much larger than they are for the corresponding neutral chain segment. Since the charge structure is localized, the enhancement factor must go through a maximum as a function of chain length. This leads to the possibility of tuning the NLO properties by varying the dopant concentration.

In principle, neutral beta materials can be charged in the same manner as gamma materials. The NLO properties of beta systems containing charged oligomers have scarcely been examined but we shall show preliminary results which suggest that further investigation is warranted.

As far as practical applications are concerned, a wide variety of devices based on NLO properties have been envisaged. The requirements for the materials that will be employed are diverse as well. One fundamental common feature is a sufficiently large NLO susceptibility. In this respect, beta materials are in a more advanced state than gamma materials. As noted earlier, an important issue for the former is preservation of the microscopic asymmetry on a macroscopic scale. This has been done successfully using organic crystals where hydrogen bonding or co-crystallization (with active or inactive compounds) controls the molecular orientation and the use of chiral species guarantees a large bulk nonlinear susceptibility, $\chi^{(2)}$. NLO susceptibilities that are one or two orders of magnitude larger than inorganic dielectrics and semiconductors, such as $LiNbO_3$ and $KTiOPO_4$, have been achieved. However, the organic crystals are not ordinarily suitable for SHG devices because of strong two-photon absorption (TPA). Organic chromophores dispersed in a polymeric host, and poled polymers, are already practical for use in electro-optical switches and modulators, but in this case thermal stability of the poling and other practical problems still remain. Langmuir–Blodgett (LB) films and self-assembled monolayers (SAMs) represent another possible approach to controlling the macroscopic order and asymmetry that has not yet come fully to fruition. There are also phase-matching conditions on the refractive indices for the incoming and outgoing waves that make a different packing required to maximize different NLO processes. For beta materials, the primary task of theory is to develop an understanding that will lead to diverse materials with a large microscopic optical nonlinearity that can be sufficiently retained under macroscopic conditions *and* will satisfy such auxiliary requirements as weak TPA and thermal stability.

For gamma materials there are also important requirements apart from large NLO susceptibility. These requirements include high laser damage thresholds as well as mechanical, thermal and environmental stability. Anisotropic heating due to high-laser-power input can create large changes in the refractive index, thereby masking the optical Kerr effect. In addition, depending upon the NLO process, excessive two- and three-photon absorption must also be avoided. In contrast with beta materials, sufficiently large microscopic susceptibilities have not yet been produced. Although π-conjugated organic polymers have the largest NLO responses observed, they are still an order of magnitude or two short of the goal. Thus the theoretical search for guiding principles that will allow this goal to be realized continues to be the highest priority.

In this section we have provided a brief overview of second- and third-order NLO property calculations for quasilinear π-conjugated oligomers or polymers and organic molecules. Some of the particular topics treated were: (i) the evolution of the property with chain length, (ii) the relative importance of vibrational as against electronic components and the connection of both to BLA, (iii) the potential for enhancement of the NLO response due to formation of charged structures, and (iv) the current status with respect to practical requirements. Within this overall picture there are many ramifications that account for the complexity of the subject as well as the opportunities for further important advances. We now turn to a detailed exploration of beta materials in section 3.2 and, finally, to gamma materials in section 3.3.

3.2. *Second-order* (*beta*) *nonlinear optical materials*

Only non-centrosymmetric systems can exhibit non-zero first hyperpolarizability values. As mentioned above, we shall concentrate on those beta materials where the asymmetry is introduced by end capping an oligomer with a D–A pair and/or by constructing an oligomer from an asymmetric building block. So far, most of the beta materials can be cast in the first category.

Even if the constituent molecules or polymers are non-centrosymmetric the first nonlinear response of the bulk, $\chi^{(2)}$, can be zero as a result of a centrosymmetric crystal packing. In addition to crystal symmetry, the unfavourable relative orientation of chromophoric entities within the unit cell will, typically, lead to a partial or complete cancellation of the nonlinear property. Some of the strategies for overcoming detrimental crystal packing effects were noted above. These will be elaborated, together with others, in section 4 where we deal with the role of the medium. Our focus in this section will be on second-order NLO properties of individual chromophores.

Numerous experimental and theoretical studies dealing with push–pull conjugated systems, that is conjugated systems end-capped with D–A pairs, have investigated the effect of the D–A pair as well as the nature and length of the conjugated linker. This subject was thoroughly reviewed by Kanis *et al.* (1994b) a couple of years ago, and therefore, we shall emphasize work that has been done since. Earlier references will be included only as necessary to provide the context for current events.

For a given polyene-like conjugated linker it has been pointed out (Ulman 1988, Cheng *et al.* 1991a, Jacquemin *et al.* 1996a) that an almost linear relation exists between β^e_L (or, for a dipole in the z direction, $\beta^e_{vec} = \frac{1}{3}\Sigma_i(\beta^e_{zii}+\beta^e_{izi}+\beta^e_{iiz}) \approx \beta^e_L$) and the difference of the Hammett σ parameters for the *para* substituent effect of each D–A pair. Several representative linkers and a variety of classical π D–A pairs have been considered. The difference in σ parameters quantifies the asymmetry of the D–A pair; the slope of the line measures the susceptibility of the π electron charge distribution. Although this relationship does provide a useful guideline, words of caution are in order. We note that firstly the quality of the fit varies depending upon the linker, secondly there is ambiguity in the choice of σ and thirdly there is an open question about the role of geometry.

Two different parameters are commonly used to represent either resonance (σ^+, σ^-) or inductive (σ_0) properties. Sometimes it is assumed that resonance is dominant for all D–A pairs (Cheng *et al.* 1991a); in other instances (Jacquemin *et al.* 1996a) a binary choice is made between σ^+/σ^- for strong D–A pairs and σ_0 for weak D–A pairs. It is preferable to make a distinction since the σ parameter should really be varied continuously between the two limits. Based on the binary choice a very good linear fit was obtained in calculations by Jacquemin *et al.* (1996a) on a $(CH{=}CH)_4$ polyene linker. However, in contrast with the experimental results of Cheng *et al.* (1991a), they used the same (artificial) polyene geometry for each D–A pair. This raises the issue of separating pure electronic contributions to the susceptibility from those that arise as a result of geometry relaxation. With a strong D–A pair the relaxation will cause a large change in the BLA of the linker and thereby have a substantial effect on β^e_L (Kanis *et al.* 1992) (see also below) or, equivalently, on the susceptibility. For weak D–A pairs the effect is small but, since they have little influence on the plot of β^e_L against σ, a good linear fit will be obtained with or without geometry relaxation. Although Kanis *et al.* showed that β^e_L can be accurately predicted using a fixed BLA, they examined only strong D–A pairs for which the BLA is approximately the same. A related study has been carried out by Marder *et al.* (1994) wherein different D–A pairs are simulated by varying a static field F applied to the model compound $(CH_3)_2N{-}(CH{=}CH)_3{-}CHO$. The geometry was allowed to relax in the presence of the (simulation) field. In this case a *nonlinear* behaviour of β^e_L against F (which may be used instead of σ) was obtained. This can be understood on the grounds that the fields considered cover a much broader range than the chemical variability of real D–A pairs. It should be noted that the results of Marder *et al.* (1994) are complicated by the fact that their method of calculating β^e_L also introduces a vibrational contribution.

Although the D–A pair is required to get a non-zero β^e_L value, the conjugated linker plays a critical role in determining the magnitude of the first hyperpolarizability. The susceptibility of an oligomeric linker depends upon both its nature and its length. The latter is the most important variable from the viewpoint of maximizing β^e_L per unit length (which we symbolize by β^e_L/N) or, almost equivalently, β^e_L per unit volume. One expects that β^e_L/N would go through a maximum as a function of chain length owing to the competition between the increase in electron delocalization and the decrease in communication between the D and A moieties as the chain is lengthened.

There have been experimental (Cheng *et al.* 1991b, Stiegman *et al.* 1991) as well as theoretical investigations of the chain length dependence of β^e_L. The majority of the calculations are of the semiempirical variety (Morley *et al.* 1987, Morley 1993, 1995, Albert *et al.* 1993) although there are also a few *ab initio* studies (Tsunekawa and Yamaguchi 1992, Jacquemin *et al.* 1996a, 1997). Semiempirical methods are advantageous because of the computational efficiency and the fact that electron correlation effects are implicitly included. On the other hand, their reliability is questionable, particularly with respect to dependence upon chain length. There are several reasons this is so. First of all, in most cases the CI space is restricted to monoexcited configurations even though it has been shown that inclusion of doubles can lead to substantial changes in β^e_L. In addition, the excited states are usually restricted to a fixed number (about 100–300) of those that are the lowest in energy. This disadvantages the longer chains with respect to shorter chains and may be the cause of the non-monotonic behaviour (Morley 1995) sometimes found for the former. Finally, the role of higher-order substitution configurations has yet to be investigated. Nonetheless, the prediction that aromatic linkers (such as planar oligo *p*-phenylenes or oligothiophenes) will yield much smaller maximum values of $\beta^e_L(0)/N$ than non-aromatic linkers (such as the linear polyenes) appears to be robust. Recent calculations (Morley 1995) predict that cumulenes will be even more potent in this regard than linear polyenes which, in turn, will be more potent than polyynes (Morley 1993). This is consistent with the order of these oligomers in terms of BLA.

All the *ab initio* calculations referenced above were done by the size-consistent CHF technique which, by definition, does not include electron correlation. It is still of interest, however, to compare the *ab initio* results of Champagne *et al.* (1997c) with those obtained semiempirically by Morley (1995) for the same $NH_2{-}(CH{=}CH)_N{-}NO_2$ chemical system. In the *ab initio* calculations, $\beta^e_L(0)/N$ is a maximum at $N = 10$ and the value at the maximum is 5·8 times that at $N = 2$; the corresponding semiempirical parameters are $N = 18$ and 15·8 respectively. Of course, including correlation in the *ab initio* treatment could change the picture and bring the two calculations into closer agreement. For particular systems a number of calculations (Velders *et al.* 1991, Sim *et al.* 1992, Velders and Teil 1992, Ågren *et al.* 1993, Mikkelsen *et al.* 1994) have found that electron correlation leads to a 15–50% increase in β^e_L within the second-order Møller–Plesset (MP2) or multiconfiguration self-consistent field (MCSCF) schemes. There are studies (see section 3.3) of how the electron correlation effect varies with chain length for the α^e_L and γ^e_L of several unsubstituted linkers. In agreement with the above calculations, electron correlation again turns out to be important, particularly for γ^e_L. The latter treatments also show that a large fraction of the effect is associated with corrections to the bond lengths along the backbone of the linker. (This is consistent with the sensitivity of β^e_L to geometry observed in the semiempirical studies of chain-length dependence). The same techniques used to obtain γ^e_L for unsubstituted oligomers can, in principle, be applied to determine $\beta^e_L(0)$ for the D–A capped oligomers. Obviously, it would be revealing to compare correlated *ab initio* results with the semiempirical calculations for $\beta^e_L(0)$.

The other two *ab initio* calculations previously mentioned deal primarily with

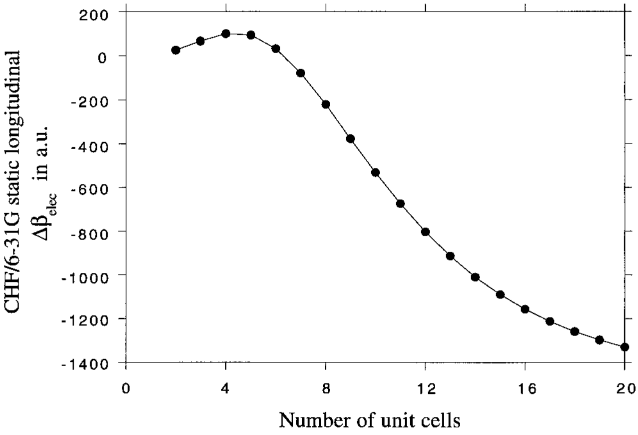

Figure 2. Static longitudinal electronic first hyperpolarizability of all-*trans* PMI chains with a BLA of 0·126 Å. Here $\Delta\beta_{\text{elec}} = [\beta^{e}_{L}(0)]_N - [\beta^{e}_{L}(0)]_{N-1}$.

asymmetric linkers containing nitrogen. Even without D–A end capping, these linkers have a non-vanishing β^{e}_{L}, but the hyperpolarizability is enhanced by capping with the NH_2–NO_2 pair. Although β^{e}_{L} is always less than that of the corresponding capped linear polyene linker, the fairly small loss in some instances may be worth the improved transparency for practical purposes. The all-*trans* polymethineimine (PMI) oligomer $-(CH{=}N)_N-$ (Jacquemin *et al.* 1996a) is an interesting case. For small chain lengths the overall asymmetry of the unsubstituted oligomeric linker (Champagne *et al.* 1997a) is dominated by the asymmetry of the chain ends. However, the asymmetry of the backbone is opposite in sign to that of the chain ends and causes the plot of β^{e}_{L}/N against N (see fig. 2) to have a characteristic 'dromedary back' shape. Thus β^{e}_{L}/N goes through an initial maximum, then changes sign and eventually reaches the asymptotic polymer limit. The magnitude of β^{e}_{L}/N at the polymer limit is much larger than at the initial maximum. For small chain lengths, the asymmetry of the NH_2–NO_2 pair acts in concert with the linker when the NO_2 group is placed at the nitrogen end of the oligomer. For longer chains, one would expect the reverse placement to be optimal and this turns out to be the case. In the infinite chain limit, of course, the placement does not matter since one approaches the value for the unsubstituted PMI polymer in either event. At the present level of calculation the infinite polymer β^{e}_{L}/N is smaller (in magnitude) than the maximum value obtained for NH_2–NO_2 capped oligomers. In fact, the value for the polymer is about the same as that of $NH_2-(CH{=}CH)_4-NO_2$.

The 'dromedary back' curve for PMI oligomers in figure 2 can be represented by writing $\beta^{e}_{L}(0)/N$ as a simple product of two functions, one arising from electron delocalization and the other from asymmetry:

$$\frac{\beta^{e}_{L}(0)}{N} = \left(m_1 + \frac{m_2 \tanh(N - m_3)}{m_4}\right)\left(1 + \frac{m_5}{N}\right). \tag{28}$$

Here $1 + m_5/N$ is the asymmetry function, in which m_5 measures the relative importance of the chain ends with respect to the backbone. The delocalization function $m_1 + m_2 \tanh(N - m_3)/m_4$ is well adapted for describing the complete chain length dependence including the gradual increase towards the asymptotic limit, as well as the inflection point that could occur at small N. In this function, $m_1 + m_2$ is the infinite polymer limit, m_3 gives the position of the inflection point, and m_2/m_1 and m_4 are associated with the amplitude and rate respectively of the evolution with chain length. The exact same treatment can be used, with different parameters, to account for the additional chain end asymmetry introduced by capping with a D–A pair.

Although the configuration interaction singles (CIS) treatment of β_L^e may suffer from some difficulties, as noted above, it has proved valuable for interpretative purposes. This follows from the fact that for many compounds a few excited states make the major contribution, at least within the singles manifold. The simplest scheme (Oudar and Chemla 1977, Oudar 1977) limits the SOS expression to a unique excited state. In the resulting two-state approximation (TSA), the static β_L^e is given by

$$\beta_L^e = \frac{6\,\Delta\mu_{gn}\,\mu_{gn}^2}{(\Delta E_{gn})^2} = \frac{6 f_{gn}\,\Delta\mu_{gn}}{(\Delta E_{gn})^3}, \tag{29}$$

where μ_{gn} is the dipole transition moment between the ground and excited state, ΔE_{gn} is the corresponding excitation energy, $\Delta\mu_{gn}$ is the dipole moment change between the ground and excited state, and $f_{gn} = \mu_{gn}^2\,\Delta E_{gn}$ is the oscillator strength. The TSA establishes a link between β_L^e and spectroscopic quantities related to the main low-lying charge transfer transition. Since the charge-transfer excited state is almost exclusively described by one basic excitation (typically highest occupied molecular orbital→ lowest unoccupied molecular orbital), it is often referred to as the two-level approximation. For a large variety of compounds, it has been shown (primarily in semiempirical calculations) that the TSA overestimates $\beta_{vec}^e (\approx \beta_L^e$ in quasilinear systems) by a factor of roughly two and that including a third state corrects the estimates to give 80% or more of the full CIS value.

When more than one excited state makes a substantial contribution, the missing state analysis of Dirk and Kuzyk (1989) can be useful. It consists of determining dimensionless quantities σ_n given by

$$\sigma_n = \frac{\beta_{tot} - \beta_n}{\beta_{tot}} \tag{30}$$

where β_{tot} is evaluated with the full SOS and β_n is determined with the nth excited state missing. Pairs of states can also be removed to obtain the effect of cross-terms. In order to illustrate the convergence of a typical CIS calculation we present in figure 3 the evolution of the static β_L^e of $NH_2{-}(CH{=}CH)_3{-}NO_2$ as a function of the number of states taken into account in the SOS expression. This *ab initio* treatment was performed using a 6-31G basis with a RHF ground state and a configuration space restricted to the 60 lowest-energy singly excited singlet states. In the same figure is displayed the results of the corresponding missing state analysis. As usual, the TSA based on the first excited state overestimates β_L^e by a factor of about two. Addition of the sixth excited state corrects this error almost completely. From the missing state analysis, removing state 1 reduces β_L^e essentially to zero. Thus the contribution due to state 6 arises as a cross-term with state 1. This work, together with that of Tsunekawa and Yamaguchi (1992), represents one of a very small number of *ab initio* CIS investigations of β_L^e.

For PMI oligomers the situation is quite different. Contrary to push–pull systems, there is a band of charge-transfer states generated by the charge transfer excitation

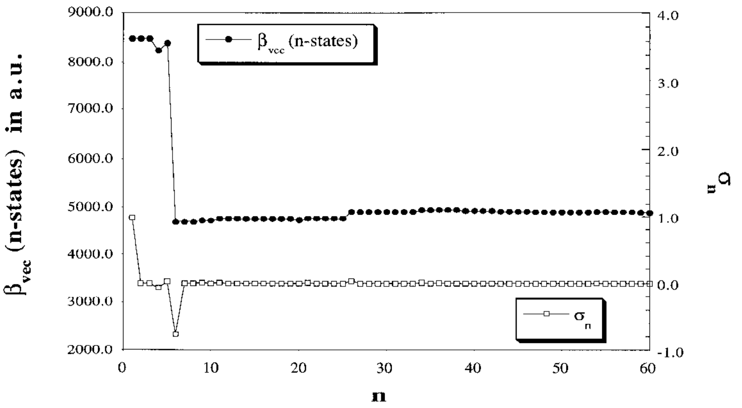

Figure 3. Static β_{vec} of NH_2–(CH=CH)$_3$–NO_2 as a function of the size of the configuration space: *n*-state approximation against missing state analysis. The calculations were performed using a 6-31G basis set with a RHF ground state and a configuration space spanning the 60 lowest-energy singly excited singlet states. σ_n is defined in equation (30).

within each –(CH=N)– unit. If the chain is small, one can develop (Jacquemin *et al.* 1996b) a reasonably accurate few-states approximation, but this approximation rapidly fails when the size of the chain is increased.

From theoretical calculations there is a consensus regarding the large potential for enhancement of $\beta_{\mathrm{L}}^{\mathrm{e}}/N$ by extending the chain length of non-aromatic linkers in push–pull systems. Because of their strong reactivity, the synthesis and isolation of such compounds have been an unrealized goal. Aromatic and/or heteroaromatic entities are often incorporated to improve stability, but they diminish the electronic delocalization and therefore $\beta_{\mathrm{L}}^{\mathrm{e}}/N$. Many different structures have been proposed and tested to find the best compromise between electronic delocalization and stability. Among these are the D–A substituted α,ω-diphenylpolyenes, α-phenylpolyenes and α,ω-diphenylacetylenes, as well as related compounds where the phenyl rings are replaced by thiophene, furan, pyrrole, etc. In these species, the departure from planarity due to inter-ring repulsion can provoke a further decrease in the NLO response.

An interesting possibility that exists for the beta materials that we have been discussing is the introduction of charges through chemical doping. Charges localized to the end groups have been considered (Kanis *et al.* 1994a, b) because of the potency of such an end group as a donor or acceptor. However, push–pull molecules where the charge is primarily localized on the linker have not been examined. It is well known that unsubstituted polymers, such as PA or polythiophene (PTh) become electrically conducting when doped (with an electron donor or acceptor) owing to charge transfer between the dopant and the chain. In the low-doping regime each chain will contain no charge, a single charge or a small number of non-interacting charges. As a model for PA, one may use an extended all-*trans* linear polyene chain. If the polyene contains a single positive charge, then recent semiempirical calculations (Larsson and Rodriguez-Monge 1996) indicate that, *in the presence of the dopant counterions*, the structure drawn *schematically* below is formed on medium–large chains:

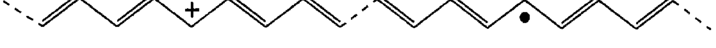

Note that the charge is localized to a region of the molecule where the normal alternating single- and double-bond pattern reverses phase. This transition region contains several carbon atoms (unlike the schematic drawing) and is known as a positive soliton. The polyene chain also contains a neutral soliton where the radical is localized. If a second positive charge is created by charge transfer with the dopant, then it is the radical electron that is transferred, leaving behind a second charged soliton.

Model calculations have been carried out to determine the value of $\gamma_L^e(0)$ for linear polyenes bearing one or two charged solitons. As we will see in the next section, the results indicate the possibility of a substantial enhancement relative to the neutral polyene. Since the charged soliton is a localized structure the enhancement factor must go through a maximum as a function of chain length or, equivalently, as a function of dopant concentration for a fixed chain length. The point to be made here is that related charged structures can occur for D–A capped linear polyenes leading to a possible enhancement of $\beta_L^e(0)$. Our own initial RHF/6-31G study (unreported as yet) on the singly charged ion with D–A = NH_2–NO_2 shows an enhancement factor that has a peak of about three for the polyene linker $(CH{=}CH)_7$. The geometrical distortion of the linker is such that almost the entire chain may be described as a transition structure with essentially equal C–C bond lengths. At the same time, the positive charge is delocalized over the entire backbone (with the exception of the NO_2 moiety) and substantially decreases the polarity of the CH=CH units.

To our knowledge no comparable studies have been undertaken for other linkers (such as PTh) or for oligomers (such as PMI) with an asymmetric repeat unit. Since the nature of the transition structure in PTh (and other aromatic or heteroaromatic) oligomers is different from the linear polyenes, the behaviour of β_L^e may be different when this oligomer is used as the linker in a D–A molecule. In PTh (as we shall see later) the geometry of the ion distorts locally to form a quinonoid-type structure, which serves as a transition between the benzenoid-type structures of the neutral regions on either side. Among other things the localized quinonoid transition region will promote planarity and thereby electronic delocalization. The effect of charging PMI oligomers (with or without D–A capping) remains to be seen and the same is true of cumulene linkers which, as neutrals, give exceptionally large β_L^e in semiempirical calculations (Morley 1995).

We turn now to the vibrational hyperpolarizabilities of the beta materials discussed in this review. As we have already seen in the introduction the vibrational contribution is expected to be negligible at optical frequencies for SHG but not for the dc Pockels effect. In the latter case the vibrational hyperpolarizability, according to equation (24), will be about a third of the static value obtained in the double-harmonic-oscillator approximation.

It has been observed for π-conjugated molecules that, in a number of instances, the calculated static vibrational hyperpolarizability is very similar in value to its electronic counterpart (Del Zoppo *et al.* 1995, Castiglioni *et al.* 1996, Champagne 1996). This observation appears to remain valid if $\beta_L^e(0)$ is inferred from experiment rather than theory, although an extrapolation of the optical EFISH measurement to zero frequency (Zuliani *et al.* 1995) is required together with other approximations. It has been argued that such a coincidence is not casual and should have an underlying physical basis. Indeed, as part of the general considerations in section 3.1 we have made the qualitative argument that both β^e and β^v are related to the BLA. The question is how to convert that qualitative argument into a quantitative relationship that will also provide a way to analyse the variations (see below) that depend upon the nature of the linker and the D–A pair.

Table 5. RHF/6-31G calculations (d functions from 6-31G* have been added on the sulphur atoms) of the $\beta_L^v(0)/\beta_L^e(0)$ ratio for α,ω-nitro-amino polyenes, polyynes and polythiophenes as a function of the number of C–C double or triple bonds.

N	NO_2–(CH=CH)$_N$–NH2	NO_2–(C≡C)$_N$–NH_2	NO_2–(Th)$_{N/2}$–NH_2
2	2·20	1·21	1·68
3	2·18	1·17	
4	2·11	1·13	2·88
5	2·01	1·10	
6	1·91		2·78
7	1·82		
8	1·74		

A first attempt, specifically for push–pull polyenes, has been made by Castiglioni *et al.* (1996). Their model includes two electronic states and one vibrational normal mode. This mode is taken to be identical with the ECC, which is the collective motion associated with BLA. The accuracy of the TSA for β^e has been discussed above. In the case of the prototype NH_2–(CH=CH)$_3$–NO_2 molecule we find that (within the TSA) an ECC-like normal mode makes the largest contribution to β_L^v, but it is less than 30% of the total. Thus it may be preferable to consider just the ECC motion without assuming that it is a normal mode, although this remains to be seen. Apart from questions that may be raised regarding the validity of the model, Bishop and Kirtman (1997) point out that the subsequent treatment neglects contributions to β_L^v that are generally larger than those retained. Thus more work must yet be done to provide a satisfactory quantitative analysis of the connections between $\beta^e(0)$ and $\beta^v(0)$ in push–pull polyenes and other polyconjugated compounds.

Some of the complexities involved in determining the relationship between $\beta^v(0)$ and $\beta^e(0)$ in polyconjugated molecules may be seen by examining the results (table 5) of our own previously unreported calculations on three prototype push–pull systems with D–A = NH_2–NO_2. For the polyenic, –(CH=CH)$_N$–, and thiophene, (Th)$_{N/2}$, linkers the values of $\beta_L^v(0)/\beta_L^e(0)$ reported in the table may be compared with the predictions of Castiglioni *et al.* (1996) which give an upper limit of two and no dependence on the type of linker or chain length. While the chain length dependence for –(CH=CH)$_N$– is less than that of either $\beta_L^e(0)/N$ or $\beta_L^v(0)/N$, it is still significant. On the other hand, the variation from one thiophene to two thiophenes is considerably larger. The data for the polyyne linker show that one must distinguish between alternating single–triple bonds and single–double bonds. Since charge doping of the linker strongly alters the bond alternation pattern of the neutral, it may not be fair to compare neutral –(CH=CH)$_N$– with the +1 ion. Nevertheless, we note that in the cation the ratio of $\beta_L^v(0)/\beta_L^e(0)$ increases from 0·57 at $N = 2$ to 0·63 at $N = 8$, whereas it varies from 2·20 to 1·74 for the corresponding neutral.

3.3 *Third-order* (*gamma*) *nonlinear optical materials*

The first hyperpolarizability of oligomers or polymers with a centre of inversion vanishes owing to symmetry. Thus the second hyperpolarizability becomes the leading nonlinear term in the expansion of the induced dipole moment as a function of applied field. We shall refer to the centrosymmetric quasilinear π-conjugated oligomers or polymers in this review as gamma materials; they are the subject of the current section. The centre of symmetry will be lost for some of the aromatic oligomers such as PTh (even in the planar all-*anti* configuration) when there is an odd number of monomer units. Nonetheless, they are meant to be included here, together with singly charged linear polyene chains that have a non-zero β because of the localized soliton that is formed.

Although most of the *ab initio* calculations to be reviewed here were done by the CHF method, there are also some correlated treatments that will be discussed. Typically, we shall be interested in either extended chains or the infinite-polymer limit. As a result, good accuracy can be achieved using a split valence basis despite the fact that such a basis is inadequate for small oligomers. The argument is that, for an extended chain, basis functions on neighbouring atoms make up for deficiencies on any given atom.

With regard to the evolution of electronic structure as a function of chain length, model oligomer calculations (Kirtman 1992) show that one should think of a new unit cell as being inserted at the centre of the chain rather than at either end. This suggests that it is preferable to estimate the hyperpolarizability of the infinite polymer per unit cell by taking the difference $[\gamma_L^e]_{N+1} - [\gamma_L^e]_N = \Delta\gamma_L^e(N)$ instead of dividing the value for the longest chain by the number of unit cells. Indeed, the former quantity converges much more rapidly with chain length to the polymer limit. The convergence is much slower, however, than the energy or geometry of the unit cell; for the hyperpolarizability an extrapolation is usually required. One mitigating factor is that the degree of convergence is determined by the number and arrangement of the conjugated bonds rather than the number of monomer units. A simple argument to this effect may be made using PA as an example. If the unit cell is taken to be $[-(CH{=}CH)-]_2$, rather than $-(CH{=}CH)-$, then saturation will be reached with a chain containing only half as many unit cells. However, there will also be fewer data points available for extrapolation, which may reduce the accuracy.

A general extrapolation procedure has now been developed (Kirtman *et al.* 1995, Champagne *et al.* 1997a) which seems to yield reliable values. The first step is to choose a variety of fitting functions. Those that have been used include the following: a power series in $1/N$ of variable order; the exponential form $a - b\exp(-cN)$; the solution of the logistic equation $a/[1 + b\exp(-cN)]$; and Padé approximants. In addition, the property per unit cell is sometimes replaced by its logarithm in carrying out a power series fit. It is our experience that no one form is best in all cases. Then, the data set is obtained by taking all points between a maximum N, namely N_{max}, and a minimum N, namely N_{min}. For a fixed N_{max} and fitting function, N_{min} is varied to determine a range over which the extrapolated hyperpolarizability (per unit cell) is stable, that is nearly constant. This is repeated, varying N_{max} and the function. The entire set of stable results obtained in this manner yield a mean value for the hyperpolarizability as well as its uncertainty.

There is one pitfall concerning the use of $\Delta\gamma_L^e(N)$ for extrapolation purposes that should be pointed out. It is sometimes difficult to obtain a smooth dependence of this quantity upon chain length, particularly for long chains. This is because of errors in the various numerical procedures that are involved. Thus, the value given below for PA was actually determined by extrapolation of $\gamma_L^e(N)$ rather than $\Delta\gamma_L^e(N)$ even though the latter converges much more rapidly with chain length.

PA is the prototype π-conjugated polymer. It has the largest $\gamma_L^e(0)$ per unit length that has been computed or measured for a real system. The first *ab initio* study of the chain length evolution was due to Hurst *et al.* (1988) who carried out static CHF/6-31G calculations of the all-*trans* linear polyenes from C_2H_4 to $C_{22}H_{24}$. This work was later extended (Kirtman *et al.* 1995) to chains containing up to 44 carbon atoms and, using the procedure described above, accurately extrapolated to obtain a polymeric value of $\gamma_L^e(N)/N = (6{\cdot}91 \pm 0{\cdot}39) \times 10^6$ au. Frequency dispersion for the most common NLO processes has recently been determined by applying the analogous TDHF approach (Hasan *et al.* 1996) for chains up to $C_{30}H_{32}$. In this case the ratio of the frequency-dependent to the static value, that is $\gamma_L^e(\omega)/\gamma_L^e(0)$, was extrapolated to the infinite-chain limit. The lowest optically allowed electronic transition frequency, at this level of treatment, was estimated from linear polarizability calculations to be about 2•8 eV. At $\omega = 0{\cdot}6$ eV ($\lambda = 206{\cdot}6$ nm) the EOKE, IDRI, dc SHG and THG values for $\gamma^e{}_L(\omega)/\gamma_L^e(0) - 1$ are 0•105, 0•221, 0•365 and 1•021 respectively. These deviate significantly from the exact low-frequency dispersion formula given by equation (11) which gives (based on EOKE as the standard) 0•105, 0•210, 0•315 and 0•630 respectively. A study of the frequency dispersion was also performed by Luo *et al.* (1995) by means of a double-direct RPA scheme (Norman *et al.* 1995) which is equivalent to the TDHF or the linear–nonlinear response function approach.

It is of interest to compare PA with other π-conjugated polymers. Any increase in the BLA such as in polyyne (PY) (Archibong and Thakkar 1993, Jaszunski *et al.* 1993, Toto *et al.* 1996) or polydiacetylene (PDA) (Kirtman and Hasan 1989) will decrease $\gamma^e{}_L(0)$ per unit length (i.e. $\gamma_L^e(0)/L$). On the other hand, polybutatriene (PBT) has a smaller BLA than PA and therefore is expected to give a larger $\gamma_L^e(0)/L$. Very large values have been calculated (Kirtman and Hasan 1989) but they must be corrected (Champagne and Öhrn 1994) to account for the soliton defect that was present at the chain end in this treatment. Just recently Perpète *et al.* (1997b) have confirmed that the CHF/6-31G value of $\gamma_L^e(0)$ for PBT is more than three times larger than that of PA. Aromaticity has been shown, in the case of polypyrrole (PPy) (Toto *et al.* 1995c), to reduce $\gamma_L^e(0)/L$ strongly. Polysilane, which is σ-conjugated, has an asymptotic value (Kirtman and Hasan 1992) that is one to two orders of magnitude smaller than PA.

It was noted in the discussion of beta materials that introducing charges onto a linear polyene chain by chemical doping or other means leads to formation of localized charged solitons and an enhancement of $\gamma_L^e(0)$. In model RHF/6-31G calculations for a chain bearing a pair of positive solitons, de Melo and Fonseca (1996) found that, at $N = 10$ (i.e. $C_{20}H_{22}$), the enhancement factor begins to increase dramatically with increasing chain length. For the longest chain examined ($N = 15$) this factor is greater than three and still growing. As noted earlier, the charged solitons are localized structures that can have no noticeable effect in the infinite-chain limit. Thus there must be a peak value for the enhancement factor which remains to be determined. This will give the doping concentration that maximizes $\gamma_L^e(0)$. Because of their mutual repulsion the positively charged solitons in these calculations are pushed towards the chain ends. In the real system, however, the solitons will be pinned by dopant counterions and the relocation and structural distortion caused by these counterions will affect $\gamma_L^e(0)$. Hence, a more realistic treatment is needed to obtain the optimum dopant concentration. On the assumption that the solitons are sufficiently far apart to be non-interacting, then each one can be modelled (omitting the structural distortion due to dopant counterions) by a chain containing an odd number of carbon atoms and a single positive charge. For this reason, calculations were also done (de Melo and Fonseca 1996) on cationic (+1) $C_{2N+1}H_{2N+3}$ chains up to $N = 11$ but, again, the lengths were not nearly sufficient to find the expected maximum in $\gamma_L^e(0)$.

The structure of the ions of conjugated oligomers or polymers with an aromatic or heteroaromatic ring as the unit cell is somewhat different from that of the linear polyenes. As an illustration a *schematic* drawing of the bond alternation pattern in the doubly positive ion of a thiophene oligomer (planar, all-*anti* configuration) is given below:

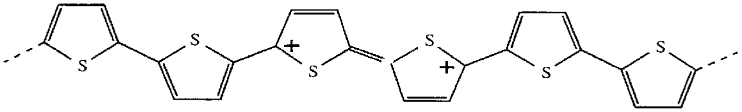

Here the two quinonoid-type rings in the centre form a localized structure, known as a bipolaron, that is flanked by benzenoid-type rings on either side. In general, unlike the schematic drawing, the bipolaron will have a width of several rings. The +1 ion has a similar alternating benzenoid–quininoid–benzenoid structure where the localized quininoid region, which contains a radical cation, is known as a polaron. Unfortunately, no calculations of $\gamma_L^e(0)$ have been reported for any polaron- or bipolaron-bearing chains. The effect of doping on the linear polarizability has been addressed at the STO-3G level (André and Delhalle 1991) and there have been quite a few treatments of the structure and vibrational spectra of bipolarons, which will be discussed shortly in connection with the vibrational hyperpolarizability.

The *ab initio* CHF determinations of $\gamma_L^e(0)$ that we have presented are sufficient to establish the order of magnitude and some general trends for isolated oligomers and polymers. Even though there have been few correlation calculations, it is clear that the latter effect can be quite important. These calculations turn out to be feasible for the static hyperpolarizability of polymers (or long chains) because the ratio of the correlated against the Hartree–Fock $\gamma_L^e(0)$ converges much more rapidly with chain length than either the numerator or denominator by itself. In PA, for example, the ratio (Toto *et al.* 1995b) is converged (for MP2/6-31G as against RHF/6-31G) to within less than 2% of the infinite chain value at $N = 4$ (i.e. octatetraene). It happens that PA is a favourable case; if the ratio is very large, then the rate of convergence can still be problematic. Under those circumstances there is another approach (see next paragraph) that has proved successful.

It is interesting that correlation increases $\gamma_L^e(0)$ substantially in all (quasilinear π-conjugated) cases considered, whereas it decreases the linear polarizability $\alpha_L^e(0)$ (although by a relatively small amount). For $\gamma_L^e(0)$ the above ratio varies (Toto *et al.* 1995a, b) from about two in PPy to about eight (rough estimate) in PY. The latter value shows slow convergence to the infinite polymer limit. Satisfactory convergence can be achieved (Toto *et al.* 1995a) by carrying out the CHF calculations at the correlated geometry, in which event the ratio is much smaller (about two). This also demonstrates that, at least in this instance, the major part of the correlation effect is due simply to the change in geometry. Note that the geometry is a property that, unlike the hyperpolarizability, converges rapidly (Kirtman *et al.* 1983) as the oligomer chain is lengthened. Finally, our conclusions about correlation should be regarded as tentative, not only because there have been few calculations but also because the basis set and the method of treating electron correlation have not been thoroughly examined.

The correlation calculations that we have discussed pertain to the static limit. Including frequency dispersion is a difficult proposition. A number of computational methods have been developed as described in §2 but, thus far, their application has been limited to relatively small systems. The simplifying assumption that the percentage dispersion correction will remain the same as it was at the Hartree–Fock level does not seem to be justified for NLO systems of the type examined here. Indeed,

Table 6. RHF/6-31G ratio of γ_L^v to $\gamma_L^e(0)$ for various optical processes at 532 nm in trisilane and pentasilane. $\gamma_L^e(0) = 14{\cdot}1 \times 10^3$ and $74{\cdot}8 \times 10^3$ au for trisilane and pentasilane respectively. Reprinted with permission from Kirtman and Hasan (1992). Copyright 1992 American Institute of Physics.

	$[\alpha^2]^{0;0}_{\omega=0}$ term	$[\mu\beta]^{0;0}_{\omega=0}$ term	Total
Si_3H_8			
Static	4·69	− 2·11	2.57
EOKE	1·56	− 1·06	0·50
Dc SHG	− 0·01	− 0·53	− 0·53
IDRI	3·12	0·0	3·12
THG	0·0	0·0	0·0
Si_5H_{12}			
Static	2·87	− 1·39	1·48
EOKE	0·95	− 0·69	0·26
Dc SHG	0·0	− 0·35	− 0·35
IDRI	1·91	0·0	1·91
THG	0·0	0·0	0·0

Sekino and Bartlett (1995) have found that this assumption considerably overshoots the mark for the longitudinal component of the EOKE in *trans*-butadiene at typical optical frequencies. Furthermore, they argue that the discrepancy will increase for longer chains because the Hartree–Fock description of the optically allowed excited states becomes worse. At this point, a study of the effect of correlation on dispersion in longer polyenes is sorely needed. There have been MCSCF calculations on the polyenes (Jaszunski *et al.* 1993) up to C_8H_2.

We have concentrated here on the *ab initio* treatment of electron correlation. In principle, the semiempirical SOS approach can be applied as well (Pierce 1989). The difficulty of having to work with a truncated configuration space is more serious than in the case of β and, again, this leads to a description that is less accurate for longer chains than for shorter chains. Not only can a plot of $\Delta\gamma_L^e$ (N) against N present spurious oscillations but also it can exhibit a maximum for medium-sized chains (Beljonne *et al.* 1993, Beljonne and Bredás 1994).

Let us now turn to the vibrational second hyperpolarizability. At the double-harmonic-oscillator level of approximation the static value $\gamma^v(0)$ is the sum of the two square brackets (cf. equation (13) and table 3): $[\alpha^2]^{0;0}_{\omega=0}$ and $[\mu\beta]^{0;0}_{\omega=0}$. From equations (25) and (26) we see that one or both of these square brackets also determines the value of γ^v (within the same approximation) for each NLO process except THG, which has a negligible vibrational contribution. In fact, IDRI depends upon $[\alpha^2]^{0;0}_{\omega=0}$; dc SHG depends upon $[\mu\beta]^{0;0}_{\omega=0}$, and EOKE depends upon a linear combination of the two. Thus two of the three major processes represent independent effects. The first-order anharmonicity terms (either electrical or mechanical) contribute only to EOKE.

The first indication that γ^v may be especially important in quasilinear conjugated systems came from calculations by Kirtman and Hasan (1992) on short polysilane oligomers which are σ conjugated rather than π conjugated. For trisilane and pentasilane the longitudinal component of both the $[\alpha^2]^{0;0}_{\omega=0}$ and $[\mu\beta]^{0;0}_{\omega=0}$ contributions are larger in magnitude than $\gamma_L^e(0)$. Since the two square brackets are of opposite sign, γ_L^v varies substantially according to the NLO process (see the ratio $\gamma_L^v/\gamma_L^e(0)$ in table 6). As a consequence, and contrary to the assumption that the more optical frequencies involved the smaller γ^v, it turns out that $|\gamma_L^v(-\omega;\omega,\omega,-\omega)| > |\gamma_L^v(0)|$ and $|\gamma_L^v(-2\omega;$

Table 7. RHF/6-31G ratio $\gamma_L^v(0)/\gamma_L^e(0)$ as a function of chain length for different π-conjugated polymers. The percentage contribution of $[\mu\beta_L]^{0;0}_{\omega=0}$ is given in parentheses. $\gamma_L^v(0)$ is evaluated within the double-harmonic approximation.

Number of C atoms	PA	PY	PDA	PBT
2	− 7·80 (2·7)	19·3 (− 5·9)		
4	2·60 (− 2·3)	1·46 (− 0·9)	2·73 (− 1·2)	− 2·02 (− 3·0)
6	1·61 (− 2·0)	1·07 (0·3)		
8	1·48 (− 1·2)	0·99 (0·6)	1·11 (0·6)	6·48 (− 5·3)
10	1·38 (− 0·4)	0·96 (0·7)		
12	1·36 (0·4)	0·95 (0·7)	1·00 (2·0)	3·84 (− 4·6)
14	1·35 (1·1)	0·94 (0·6)		
16	1·34 (1·7)		0·93 (2·9)	3·46 (− 3·7)
18	1·34 (2·3)			
20	1·34 (2·8)			

$\omega, \omega, 0)| > |\gamma_L^v(-\omega; \omega, 0, 0)|$. (As an aside we note that at 532 nm the infinite-frequency approximation is satisfied within a fraction of a per cent.) The largest contributions to $[\mu\beta]^{0;0}_{\omega=0}$ originate from hydrogen-wagging motions, which are known to generate a substantial delocalized polarization of the electron density (Champagne *et al.* 1995). For $[\alpha^2]^{0;0}_{\omega=0}$ the major contributions are provided by other longitudinal motions, including a vibration that becomes (Kirtman *et al.* 1996) the collective longitudinal acoustic mode in longer chains.

In non-aromatic π-conjugated oligomers or polymers, the $[\alpha^2]^{0;0}_{\omega=0}$ term is much larger in magnitude than $[\mu\beta]^{0;0}_{\omega=0}$ (table 7). Therefore, within the double-harmonic-oscillator approximation, the various γ_L^v are given accurately by $\gamma_L^v(0) = 3\gamma_L^v(-\omega; \omega, 0, 0) = \frac{3}{2}\gamma_L^v(-\omega; \omega, \omega, -\omega) = [\alpha^2{}_L]^{0;0}_{\omega=0}$ and $\gamma_L^v(-2\omega; \omega, \omega, 0) = \gamma_L^v(-3\omega; \omega, \omega, \omega) = 0$. A comparison of PBT and PDA (Perpète *et al.* 1997b) in table 7 shows that the degree of BLA can strongly influence the ratio $\gamma_L^v(0)/\gamma_L^e(0)$. Of the four polymers, PBT has the smallest bond length differences and the largest value for this ratio. In PA, $\gamma_L^v(0)$ rapidly saturates towards a value 34% larger than $\gamma_L^e(0)$ (Champagne *et al.* 1997b, Champagne and Kirtman 1997a) whereas for PY (Perpète *et al.* 1997a) and PDA the asymptotic $\gamma_L^v(0)$ is roughly 90% of $\gamma_L^e(0)$. A further analysis of the chain length dependence has been presented by Perpète *et al.* (1997b).

In these π-conjugated oligomers, the most important normal modes are in-phase unit cell ($k = 0$) vibrations which involve the BLA of the entire backbone. As mentioned previously the coordinate which describes this BLA motion is known as the ECC and, according to the nature of the chain, it mixes with other $k = 0$ in-plane motions to form various normal modes. In PA chains, two normal modes contribute more than 85% of $[\alpha^2]^{0;0}_{\omega=0}$; they are both admixtures of hydrogen-wagging and ECC motions (Champagne *et al.* 1997b). The hydrogen-wagging component is predominant in each case but the magnitude of the linear polarizability derivative $\partial\alpha_L/\partial Q$ is determined (Kirtman *et al.* 1996) primarily by the quasi-ECC motion (which differs from the ECC motion due to chain end effects described below). In fact, the proportion of hydrogen wagging is larger for the lower-frequency mode ($\omega_a = 1320$ cm^{-1}) than the higher-frequency mode ($\omega_a = 1860$ cm^{-1}) but $[\alpha^2]^{0;0}_{\omega=0} \approx (\partial\alpha_L/\partial Q_a)^2\ \omega_a^{-2}$ is larger for the latter. The carbon and hydrogen motions are parallel in the 1320 cm^{-1} vibration but antiparallel in the higher-frequency mode.

Because of the simple structure of PY chains, only one normal mode (ω_v = 2590–2570 cm^{-1}) contributes significantly (95%) to $[\alpha^2]^{0;0}_{\omega=0}$ (Perpète *et al.* 1997a). It is a quasi-ECC mode where, as in PA, there is a substantial fall-off of the BLA at the chain extremities. In PDA and PBT, two modes characterized by different types of BLA lead to substantial $[\alpha^2]^{0;0}_{\omega=0}$ contributions (Perpète *et al.* 1997b). The lower-frequency mode (ω_a = 1820–1800 cm^{-1}) in PDA yields 30–33% of the total $[\alpha^2]^{0;0}_{\omega=0}$. It corresponds to a single–double BLA whereas the higher-frequency mode (ω_a = 2505–2490 cm^{-1}) corresponds to a single–triple BLA and contributes 40–45% of the total. The situation is similar in PBT. Two vibrational modes having frequencies of about 1250 cm^{-1} and 2330–2270 cm^{-1} yield 30–35% and 46–48% respectively of the total $[\alpha^2]^{0;0}_{\omega=0}$. Again, the lower-frequency mode is mainly associated with a single–double BLA; the higher-frequency vibration corresponds to a double–double BLA. It should be noted that the relevant vibrational frequencies all lie in the medium–high range, that is from about 1250 to 2600 cm^{-1} or 0·15 to 0·32 eV. Thus the response times are about one order of magnitude slower than electronic response times.

The results in table 7 demonstrate that the $\gamma^{\mathrm{v}}_{\mathrm{L}}(0)/\gamma^{\mathrm{e}}_{\mathrm{L}}(0)$ ratio depends significantly upon the chemical nature and length of the conjugated chain. This contrasts with the conclusions of Del Zoppo *et al.* (1992, 1993) and Castiglioni *et al.* (1995) who proposed that $\gamma^{\mathrm{v}}(0)$ and $\gamma^{\mathrm{e}}(0)$ should be regarded as essentially identical because of the similarity that they found between $\log \gamma^{\mathrm{v}}(0)$ and $\log \gamma^{\mathrm{e}}(0)$ for various conjugated systems including PA and PTh oligomers. It is also important to remember that a particular $\gamma^{\mathrm{v}}(0)$ will give quite different values for the vibrational NLO response depending upon the process. Finally, the validity of the assumption made by Del Zoppo *et al.* and Castiglioni *et al.* that $[\mu\beta]^{0;0}_{\omega=0}$ will always be negligible still remains to be established.

For PA chains, the first-order vibrational anharmonicity correction to the EOKE has been obtained using the finite-field relaxation procedure (Bishop *et al.* 1995). It turns out to be on the order of 10% or less (Champagne and Kirtman 1997a) except for butadiene, in which case the correction is 22%.

To our knowledge the square-bracket terms that contribute to $\gamma^{\mathrm{v}}(0)$ in the double-harmonic-oscillator approximation have not been evaluated for any of the charged structures that were discussed earlier in this section. The static vibrational linear polarizability $\alpha^{\mathrm{v}}_{\mathrm{L}}(0)$ has been determined (Champagne *et al.* 1997c) for polyene chains bearing a positive soliton. Once again, these calculations were done at the RHG/6-31G level using the $C_{2N+1}H^{+}_{2N+3}$ polyene ions as a model. The expression for $\alpha^{\mathrm{v}}_{\mathrm{L}}$, in the double-harmonic-oscillator approximation, is the same as that given for $[\mu\beta]^{0,0}$ in table 4 except for the following changes:

$$\tfrac{1}{6} \rightarrow \tfrac{1}{2};\ P_{-\sigma,1,2,3} \rightarrow P_{-\sigma,1};\ \beta\gamma\delta \rightarrow \beta.$$

Thus each mode contributes an amount proportional to the square of the dipole derivative or the infrared intensity of that mode. For the longest chain considered ($C_{29}H^{+}_{31}$), $\alpha^{\mathrm{v}}_{\mathrm{L}}(0)$ was found to be over 150 times larger than the vibrational polarizability in neutral $C_{28}H_{30}$. It is also over 4·5 times larger than the static $\alpha^{\mathrm{e}}_{\mathrm{L}}(0)$ for the same $C_{29}H^{+}_{31}$ chain. From the data the ratio $\alpha^{\mathrm{v}}_{\mathrm{L}}(0)/\alpha^{\mathrm{e}}_{\mathrm{L}}(0)$ will clearly increase initially as the chain is further lengthened. What will happen when one of the dipole derivatives is replaced by a β derivative to yield the $[\mu\beta]^{0;0}_{\omega=0}$ square-bracket term is an open question.

Most of the quantities that appear in the formulae for the square-bracket terms in table 4 also occur in *ab initio* treatments of Raman and infrared spectra. As we have seen above, the $[\mu\beta]^{0;0}_{\omega=0}$ term is proportional to the square root of the product of the infrared and hyper Raman intensities, while the $[\alpha^2]^{0;0}_{\omega=0}$ term is directly proportional to the Raman intensity. Raman (and infrared) intensities have been calculated (Villar *et* *al.* 1988a, b) for $C_{2n+1}H^{+}_{2n+3}$ chains, but unfortunately the data reported are insufficient to determine $[\alpha^2]^{0;0}_{\omega=0}$. Ehrendorfer and Karpfen (1994, 1995) have carried out a set of vibrational spectra calculations for positive bipolarons on oligothiophenes chains (planar all-*anti* conformation). They predict a large enhancement of Raman intensities (depending upon the chain length), together with an even more striking increase in infrared intensities, compared with the corresponding neutral. (The Raman enhancement is primarily a geometrical effect due to the quininoid structure whereas the infrared enhancement is due primarily to the charge.) This suggests that one or both of the zeroth-order square-bracket terms that occur in $\gamma^{\mathrm{v}}_{\mathrm{L}}(0)$ may be exceptionally large. Up to this point, no calculations for (singly charged) polarons on oligothiophene chains have been made.

The state of knowledge regarding other prototype aromatic (or hetero-aromatic) oligomers, such as oligo-*p*-phenylenes and oligo-pyrroles, is more primitive. An important generic question concerns the possible deviation from planarity due to torsional displacements about C–C inter-ring bonds. For the neutrals the existing evidence indicates that, in all cases, the oligomers are planar or nearly planar in the solid state.

4. Role of the medium

Up to this point we have focused on individual molecular or polymeric chains. In the real system these chains will interact with the surrounding medium. For beta materials in the solid state the relative orientation of the chromophores is crucial for $\chi^{(2)}$. Although this one particular aspect has been extensively considered, the role of the solid state medium in determining bulk nonlinear response has otherwise been largely ignored.

Recently, the effect of liquid solvents on the NLO properties of beta chromophores has come under scrutiny because the measurements that one wants to compare with computational results are normally made in solution. Current theoretical treatments are based on the reaction field model where the solvent is described as a polarizable continuum characterized by a macroscopic dielectric constant. The chromophore, which is taken to be embedded in a cavity, induces an electric field in the continuum and that field, in turn, reacts upon the chromophore, producing a solute–solvent interaction term that is incorporated into the Hamiltonian. There are many issues involved in applying this model such as the size and shape of the cavity, the discontinuity at the cavity boundary surface, the order of the multipolar field expansion, the relative importance of changes in transition and permanent dipole moments against excitation energies, and whether one or more solvent shells should be included (see below) in the cavity. Many of these aspects have been addressed in recent papers (van Duijnen and de Vries 1995, Mikkelsen *et al.* 1994) and review articles (Bishop 1994b, Tomasi and Perisco 1994). We do not wish to dwell upon them here. Suffice it to say that the effects in push–pull systems on the electronic hyperpolarizability can be substantial; calculated increases by a factor of up to two or three have been reported (Mikkelsen *et al.* 1994, Di Bella *et al.* 1994) and they, at least partially, account for earlier discrepancies between theory and experiment. No studies of the solvent effect on the vibrational hyperpolarizability have yet appeared.

Let us turn now to beta materials in a solid-state environment. We have already observed that the relative orientation of the chromophores is crucial for $\chi^{(2)}$. It has been shown (Oudar and Zyss 1982, Zyss and Oudar 1982) that, in a crystal, unfavourable dipolar orientations within the unit cell and phase-matching requirements lead typically to partial or complete cancellation of the individual molecular contributions so that, at most, a quarter to a third of the possible $\chi^{(2)}$ response remains. D–A π-conjugated chromophores, such as those discussed in this review, normally exhibit large permanent dipole moments oriented primarily along the longitudinal axis. Thus electrostatic dipole–dipole interactions will strongly favour antiparallel centrosymmetric (or nearly centrosymmetric) structures. The use of weaker D–A groups or the addition of substitutents to the chromophore can avoid this symmetric packing. However, both strategies decrease the NLO response in the direction of the dipole moment, in the former case because the longitudinal hyperpolarizability is reduced and in the latter case because the dipole moment is no longer parallel to the charge transfer axis. Another possibility is to create three-dimensional structures with relatively low packing density, such as LB films or SAMs, so that the chromophores are weakly interacting. Co-crystallization can serve the same purpose. Alternatively, hydrogen bonding is of particular interest as a means of stabilizing structures where the permanent dipoles are parallel despite the dipole–dipole interactions which favour an antiparallel configuration. Such a parallel arrangement is maintained by a network of hydrogen bonds in crystals of *N*-(4-nitrophenyl)-(L)-prolinol. In these crystals the D–A chromophores are in vertical stacks where the immediate neighbours (within a stack) are horizontally translated with respect to one another. Semiempirical calculations (Di Bella *et al.* 1992) reveal that translation by about one molecular length is optimum for the electronic NLO response. Again, the vibrational NLO has not been considered.

There has been much less work regarding the effect of the medium on gamma materials. A pair of *ab initio* model studies for polyacetylene in the solid state have been carried out with interesting results. In a stretched fibre of PA each polymer chain is surrounded by a hexagon of nearest neighbours at an experimentally known distance and orientation. Two of the neighbouring chains are parallel to the central one; the other four are quasi perpendicular. *Ab initio* RHF/6-31G supermolecule calculations (Kirtman 1996), using short linear polyene models, show a dramatic reduction (about 85%) in $\gamma_L^e(0)$ due to interactions with the entire set of nearest neighbours. The percentage reduction due to interaction with one or two neighbours (which are the only cases that have been tested thus far) remains remarkably constant when the chain length is varied or electron correlation is included by any one of several methods. Furthermore, the basis set superposition error is negligible despite the small size of the basis that was employed. As a caveat we should note that these calculations were done with an in-phase arrangement for the single and double bonds of adjacent quasiperpendicular chains, whereas it is now thought the arrangement is most likely out of phase. An earlier semiempirical treatment (McWilliams and Soos 1991), in contrast with the *ab initio* results, found a non-monotonic behaviour as more nearest neighbours are added and an overall increase in $\gamma_L^e(0)$ for the entire shell. Further *ab initio* investigation of longer polyenes and larger basis sets is in progress.

An explanation of the large reduction in $\gamma_L^e(0)$ described above has yet to be given. One possible approach is through symmetry-adapted perturbation theory (Jeziorski *et al.* 1994) which provides an analysis (Moszynski *et al.* 1996) based on polarization, exchange, induction and dispersion contributions. Another remaining question is whether the effect of nearest neighbours dominates, as expected, over more distant neighbours. This is being investigated by reaction field methods where the more distant neighbours are represented by a dielectric continuum or by a combination of dielectric continuum and intermolecular potential.

We have also begun to investigate (Champagne and Kirtman 1997b) the effect of solid state packing upon $\gamma_L^v(0)$, particularly the $[\alpha^2]^{0;0}_{\omega=0}$ term which makes the major contribution. Clusters of two or three small linear polyene chains were again considered. There are two effects: one is due to the intermolecular vibrational potential and the other arises from modifications of the intramolecular potential induced by changes in the electronic structure. The former is reflected in the contribution of low-frequency vibrations and depends strongly upon the relative orientation of the chains as well as their size. Although the effect is substantial for small chains, as the chain is lengthened it becomes small in comparison with the intramolecular component. On the other hand, solid-state packing decreases $[\alpha^2]^{0;0}_{\omega=0}$ for the two dominant intramolecular hydrogen-wagging – ECC modes by about 28% for two chains and 40% for three chains, with only a slight dependence upon the chain length or the relative orientation. These reductions are very similar in magnitude to what was found for $\gamma_L^e(0)$.

Clearly, we are just beginning to learn about the quantitative role of the medium in determining NLO properties in the solid state. PA is of great interest but we need to know more about π-conjugated systems containing aromatic (or heteroaromatic) rings, charged structures (with the dopant included), D–A charge transfer molecules, etc. This is not to mention the effect of disorder and of the various structural defects and impurities that may be present.

Acknowledgments

The authors are indebted to Jean-Marie André, David M. Bishop, Celso De Melo, Denis Jacquemin and Eric A. Perpète for many fruitful discussions (names given in alphabetical order). B.C. thanks the Belgian national Fund for Scientific Research for his Research Associate position. Calculations have been performed on the IBM RS6000 cluster of the Namur Scientific Computing Faculty and the Maui High Performance Computer Center. The authors gratefully acknowledge the financial support of the FNRS–FRFC, the Loterie Nationale for the convention No. 9.4593.92, the FNRS within the framework of the Action d'Impulsion à la Recherche Fondamentale of the Belgian Ministry of Science under the convention D.4511.93, and the Belgian National Interuniversity Research Program on Sciences of Interfacial and Mesoscopic Structures (PAI–IUAP No. P3-049).

References

Ågren, H., Vahtras, H. O., Koch, H., Jørgensen, P., and Helgaker, T., 1993, *J. chem. Phys.*, **98**, 6417.

Aiga, F., Sasagne, K., and Itoh, R., 1993, *J. chem. Phys.*, **99**, 3779.

Albert, I. D. L., Pugh, D., and Morley, J., 1994, *J. chem. Soc.*, *Faraday Trans.*, **90**, 2617.

André, J. H., and Delhalle, J., 1991, *Chem. Rev.*, **91**, 843.

Archibong, E. F., and Thakkar, A. J., 1993, *J. chem. Phys.*, **98**, 8324.

Beljonne, D., and Brédas, J. L., 1994, *Phys. Rev.* B, **50**, 2841.

Beljonne, D., Shuai, Z., and Brédas, J. L., 1993, *J. chem. Phys.*, **98**, 8819.

Bishop, D. M., 1990, *Rev. mod. Phys.*, **62**, 343; 1994a, *J. chem. Phys.*, **100**, 6535; 1994b, *Int. Rev. phys. Chem.*, **13**, 21.

Bishop, D. M., and Dalskov, E. K., 1996, *J. chem. Phys.*, **104**, 1004.

Bishop, D. M., and De Kee, D. W., 1996a, *J. chem. Phys.*, **104**, 9876; 1996b, *ibid.*, **105**, 8247.

Bishop, D. M., Hasan, M., and Kirtman, B., 1995, *J. chem. Phys.*, **103**, 4157.

Bishop, D M., and Kirtman, B., 1991, *J. Chem. Phys.*, **95**, 2646; 1992, *ibid.*, **97**, 5255; 1997, *Phys. Rev.* B, **55**, BISHOP, D. M., KIRTMAN, B., and CHAMPAGNE, B., 1997, *J. chem. Phys.* (to be published).

BISHOP, D. M., KIRTMAN, B., KURTZ, H. A., and RICE, J. E., 1993, *J. chem. Phys.*, **98**, 8024.

CASTIGLIONI, C., DEL ZOPPO, M., and ZERBI, G., 1993, *J. Raman Spectrosc.*, **24**, 485; 1996, *Phys. Rev.* B, **53**, 13 319.

CASTIGLIONI, C., DEL ZOPPO, M., ZULIANI, P., and ZERBI, G., 1995, *Synth. Metals*, **74**, 171.

CHAMPAGNE, B., 1996, *Chem. Phys. Lett.*, **261**, 57.

CHAMPAGNE, B., DEUMENS, E., and ÖHRN, Y., 1997c, *J. chem. Phys.* (submitted).

CHAMPAGNE, B., JACQUEMIN, D., ANDRÉ, J. M., and KIRTMAN, B., 1997a, *J. phys. Chem.* A, **101**, 3158.

CHAMPAGNE, B., and KIRTMAN, B., 1997a, *J. chem. Phys.* (to be submitted); 1997b, *Chem. Phys. Lett.* (to be submitted).

CHAMPAGNE, B., and ÖHRN, Y., 1994, *Chem. Phys. Lett.*, **217**, 551.

CHAMPAGNE, B., PERPÈTE, E., and ANDRÉ, J. M., 1994, *J. chem. Phys.*, **101**, 10 796.

CHAMPAGNE, B., PERPÈTE, E. A., ANDRÉ, J. M., and KIRTMAN, B., 1995, *J. chem. Soc., Faraday Trans.*, **91**, 1641; 1997b, *Synth. Metals*, **85**, 1047.

CHENG, L. T., TAM, W., STEVENSON, S. H., MEREDITH, G. R., RIKKEN, G., and MARDER, S. R., 1991A, *J. phys. Chem.*, **95**, 10 631.

CHENG, L. T., TAM, W., MARDER, S. R., STIEGMAN, A. E., RIKKEN, G., and SPANGLER, C. W., 1991b, *J. phys. Chem.*, **95**, 10 643.

DEL ZOPPO, M., CASTIGLIONI, C., VERONELLI, M., and ZERBI, G., 1993, *Synth. Metals*, **57**, 3919.

DEL ZOPPO, M., CASTIGLIONI, C., and ZERBI, G., 1995, *Nonlinear Optics*, **9**, 73.

DEL ZOPPO, M., CASTIGLIONI, C., ZERBI, G., RUI, M., and GUSSONI, M., 1992, *Synth. Metals*, **51**, 135.

DE MELO, C. P., and FONSECA, T. L., 1996, *Chem. Phys. Lett.*, **261**, 28.

DI BELLA, S., MARKS, T. J., and RATNER, M. A., 1994, *J. Am. chem. Soc.*, **116**, 4440.

DI BELLA, S., RATNER, M. A., and MARKS, T. J., 1992, *J. Am. chem. Soc.*, **114**, 5842.

DIRK, C. W., and KUZYK, M. G., 1989, *Phys. Rev.* A, **39**, 1219.

EHRENDORFER, CH. and KARPFEN, A., 1994, *J. phys. Chem.*, **98**, 7492; 1995, *ibid.*, **99**, 5341.

ELLIOTT, D. S., and WARD, J. F., 1984, *Molec. Phys.* **51**, 45.

HASAN, M., KIM, S. J., TOTO, J. L., and KIRTMAN, B., 1996, *J. chem. Phys.*, **105**, 186.

HURST, G. J. B., DUPUIS, M., and CLEMENTI, E., 1988, *J. chem. Phys.* **89**, 385.

IWATA, S., 1983, *Chem. Phys. Lett.*, **102**, 544.

JACQUEMIN, D., CHAMPAGNE, B., and ANDRÉ, J. M., 1996a, *Synth. Metals*, **80**, 205.

JACQUEMIN, D., CHAMPAGNE, B., ANDRÉ, J. M., and KIRTMAN, B., 1996b, *Chem. Phys.*, **213**, 217; 1997, *J. Chem. Phys.* (to be published).

JASZUNSKI, M., JØRGENSEN, P., KOCH, H., ÅGREN, H., and T. HELGAKER, 1993, *J. Chem. Phys.* **98**, 7229.

JEZIORSKI, B., MOSZYNSKI, R., and SZALEWICZ, K., 1994, *Chem. Rev.*, **94**, 1887.

KANIS, D. R., MARKS, T. J., and RATNER, M. A., 1992, *Int. J. quant. Chem.*, **43**, 61. 1994a, *Molec. Crystals liquid Crystals Sci. Technol.* B, **6**, 317.

KANIS, D. R., RATNER, M. A., and MARKS, T. J., 1994b, *Chem. Rev.*, **94**, 195.

KARNA, S. P., and DUPUIS, M., 1991, *J. comput. Chem.*, **12**, 487.

KIRTMAN, B., 1992, *Int. J. quant. Chem.*, **43**, 147; 1996, *Theoretical and Computational Modeling of NLO and Electronic Materials*, American Chemical Society Symposium Series, Vol. 628, edited by S. P. Karna and A. T. Yeates (Washington, DC: American Chemical Society), p. 58.

KIRTMAN, B., and BISHOP, D. M., 1990, *Chem. Phys. Lett.*, **175**, 601.

KIRTMAN, B., CHAMPAGNE, B., and ANDRÉ, J. M., 1996, *J. chem. Phys.*, **104**, 4125.

KIRTMAN, B., and HASAN, M., 1989, *Chem. Phys. Lett.*, **157**, 123; 1992, *J. chem. Phys.*, **96**, 470.

KIRTMAN, B., NILSSON, W. B., and PALKE, W. E., 1983, *Solid state Commun.*, **46**, 791.

KIRTMAN, B., TOTO, J. L., ROBINS, K. A., and HASAN, M., 1995, *J. chem. Phys.*, **102**, 5350.

LARSSON, S., and RODRIGUEZ-MONGE, L., 1996, *Int. J. quant. Chem.*, **58**, 517.

LINDERBERG, J. and ÖHRN, Y., 1973, *Propagators in Quantum Chemistry* (New York: Academic Press).

LUO, Y., ÅGREN, H., KOCH, H., JØRGENSEN, P., and HELGAKER, T., 1995, *Phys. Rev.* B, **51**, 14 949.

MARDER, S. R., GORMAN, C. B., MEYERS, F., BOURHILL, G., BRÉDAS, J. L., and PIERCE, B. M., 1994, *Science*, **265**, 632.

McWilliams, P. C. M., and Soos, Z. G., 1991, *J. chem. Phys.*, **95**, 2127.

Mikkelsen, K. V., Luo, Y., Ågren, H., and Jørgensen, P., 1994, *J. chem. Phys.*, **100**, 8240; 1995, *ibid.*, **102**, 9362.

Morley, J., 1993, *Int. J. quant. Chem.*, **46**, 19; 1995, *J. phys. Chem.*, **99**, 10166.

Morley, J. O., Docherty, V. J., and Pugh, D., 1987, *J. chem. Soc., Perkin Trans. II*, 1351.

Moszynski, R., Heijman, T. G. A., Wormer, P. E. S., and Van Der Avoird, A., 1996, *J. chem. Phys.*, **104**, 6997.

Norman, P., Jonsson, D., Vahtras, O., and Ågren, H., 1995, *Chem. Phys. Lett.*, **242**, 7.

Oddershede, J., 1987, *Adv. chem. Phys.*, **69**, 201.

Olsen, J., and Jørgensen, P., 1985, *J. chem. Phys.* **82**, 3235.

Orr, B. J., and Ward, J. F., 1971, *Molec. Phys.*, **20**, 513.

Oudar, J. L., 1977, *J. chem. Phys.* **67**, 446.

Oudar, J. L., and Chemla, D. S., 1977, *J. chem. Phys.*, **66**, 2664.

Oudar, J. L., and Zyss, J., 1982, *Phys. Rev.* A, **26**, 2016.

Perpète, E. A., Champagne, B., André, J. M., and Kirtman, B., 1997a, *J. molec. Struct.* (*Theochem*) (to be published).

Perpète, E. A., Champagne, B., and Kirtman, B., 1997b, *J. chem. Phys.* (to be published).

Pierce, B. M., 1989, *J. chem. Phys.*, **91**, 791.

Rice, J. E., and Handy, N. C., 1991, *J. chem. Phys.*, **94**, 4959.

Sasagne, K., Aiga, F., and Itoh, R., 1993, *J. chem. Phys.*, **99**, 3738.

Sekino, H., and Bartlett, R. J., 1986, *J. chem. Phys.*, **85**, 976; 1991, *ibid.*, **94**, 3665; 1992, *Int. J. quant. Chem.*, **43**, 119; 1993, *J. chem. Phys.*, **98**, 3022; 1995, *Chem. Phys. Lett.*, **234**, 87.

Sim, F., Chin, S., Dupuis, M., and Rice, J. E., 1993, *J. phys. Chem.*, **97**, 1158.

Spackman, M. A., 1996, *Molec. Phys.*, **88**, 1109.

Stanton, J. F., and Bartlett, R. J., 1993, *J. chem. Phys.*, **99**, 5178.

Stiegman, A. E., Graham, E., Perry, K. J., Khundkar, L. R., Cheng. L. T., and Perry, J. W., 1991, *J. Am. chem. Soc.*, **113**, 7658.

Tomasi, J., and Persico, M., 1994, *Chem. Rev.*, **94**, 2027.

Toto, J. L., Toto, T. T., and De Melo, C. P., 1995a, *Chem. Phys. Lett.* **245**, 660.

Toto, J. L., Toto, T. T., de Melo, C. P., Hasan, M., and Kirtman, B., 1995b, *Chem. Phys. Lett.*, **244**, 59.

Toto, J. L., Toto, T. T., de Melo, C. P., Kirtman, B., and Robins, K. A., 1996, *J. chem. Phys.*, **104**, 8586.

Toto, J. L., Toto, T. T., de Melo, C. P., and Robins, K. A., 1995c, *J. chem. Phys.* **102**, 8048.

Tsunekawa, T., and Yamaguchi, K. 1992, *J. phys. Chem.*, **96**, 10268.

Ulman, A., 1988, *J. phys. Chem.*, **92**, 2385.

van Duijnen, P. Th., and de Vries, A. H., 1995, *Int. J. quant. Chem.* **S, 29**, 523.

Velders, G. J. M., and D. Feil, 1992, *J. phys. Chem.*, **96**, 10725.

Velders, G. J. M., Gillet, J. M., Becker, P. J., and Feil, D., 1991, *J. phys. Chem.*, **95**, 8601.

Villar, H. O., Dupuis, M., and Clementi, E., 1988a, *J. chem. Phys.*, **88**, 5252; 1988b, *Phys. Rev.* B, **37**, 2520.

Zuliani, P., Del Zoppo, M., Castiglioni, C., Zerbi, G., Andraud, C., Brotin, T., and Collet, A., 1995, *J. Phys. Chem.*, **99**, 16242.

Zyss, J., and Oudar, J. L., 1982, *Phys. Rev.* A, **26**, 2028.